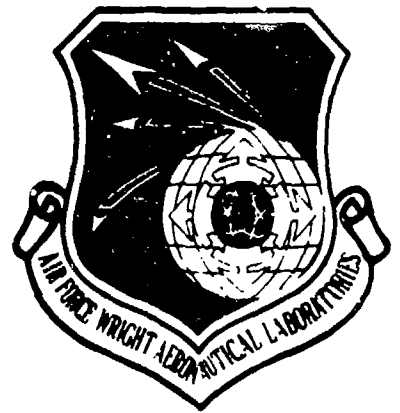


AD A106129

LEVEL

12



AFWAL-TR-81-2049

TEST AND EVALUATION OF U.V. FIBER OPTICS
FOR APPLICATION TO AIRCRAFT FIRE DETECTOR SYSTEMS

HTL INDUSTRIES, INC.
ADVANCED TECHNOLOGY DIVISION
1800 HIGHLAND AVENUE
DUARTE, CALIFORNIA 91010

JUNE 1981

FINAL REPORT FOR PERIOD: MAY 1980 - MARCH 1981

APPROVED FOR PUBLIC RELEASE; DISTRIBUTION UNLIMITED

AERO PROPULSION LABORATORY
AIR FORCE WRIGHT AERONAUTICAL LABORATORIES
AIR FORCE SYSTEMS COMMAND
WRIGHT-PATTERSON AIR FORCE BASE
DAYTON, OHIO

DTIC FILE COPY

DTIC
S
JUN 27 1981
A

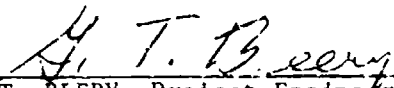
81 10 27 280

NOTICE

When Government drawings, specifications, or other data are used for any purpose other than in connection with a definitely related Government procurement operation, the United States Government thereby incurs no responsibility nor any obligation whatsoever; and the fact that the government may have formulated, furnished, or in any way supplied the said drawings, specifications, or other data, is not to be regarded by implication or otherwise as in any manner licensing the holder or any other person or corporation, or conveying any rights or permission to manufacture use, or sell any patented invention that may in any way be related thereto.

This report has been reviewed by the Office of Public Affairs (ASD/PA) and is releasable to the National Technical Information Service (NTIS). At NTIS, it will be available to the general public, including foreign nations.

This technical report has been reviewed and is approved for publication.



G.T. BEERY, Project Engineer
Fire Protection Branch
Fuels and Lubrication Division
Aero Propulsion Laboratory



ROBERT G. CLODFELTER, Chief
Fire Protection Branch
Fuels and Lubrication Division
Aero Propulsion Laboratory

FOR THE COMMANDER



ROBERT D. SHERRILL, Chief
Fuels and Lubrication Division
Aero Propulsion Laboratory

"If your address has changed, if you wish to be removed from our mailing list, or if the addressee is no longer employed by your organization please notify AFWAL/POSH. W-PAFB, OH 45433 to help us maintain a current mailing list".

Copies of this report should not be returned unless return is required by security considerations, contractual obligations, or notice on a specific document.

19 REPORT DOCUMENTATION PAGE		READ INSTRUCTIONS BEFORE COMPLETING FORM
1. REPORT NUMBER AFWAL-TR-81-2049	2. GOVT ACCESSION NO. AD-A106129	3. RECIPIENT'S CATALOG NUMBER
4. TITLE (and Subtitle) TEST AND EVALUATION OF U.V. FIBER OPTICS FOR APPLICATION TO AIRCRAFT FIRE DETECTOR SYSTEMS		5. TYPE OF REPORT & PERIOD COVERED Final Report 3 May 81
7. AUTHOR(s)		6. PERFORMING ORG. REPORT NUMBER
9. PERFORMING ORGANIZATION NAME AND ADDRESS HTL Industries, Inc. Advanced Technology Division Duarte, Calif 91010		8. CONTRACT OR GRANT NUMBER(s) F33615-80-C-2042
11. CONTROLLING OFFICE NAME AND ADDRESS Aero Propulsion Laboratory (AFWAL/POSH) Air Force Wright Aeronautical Laboratories Wright-Patterson AFB, Ohio 45433		10. PROGRAM ELEMENT, PROJECT, TASK AREA & WORK UNIT NUMBERS 62203F 3048 07/91
14. MONITORING AGENCY NAME & ADDRESS (if different from Controlling Office)		12. REPORT DATE June 1981
		13. NUMBER OF PAGES 56
		15. SECURITY CLASS. (of this report) Unclassified
		15* DECLASSIFICATION DOWNGRADING SCHEDULE
16. DISTRIBUTION STATEMENT (of this Report) APPROVED FOR PUBLIC RELEASE; DISTRIBUTION UNLIMITED		
17. DISTRIBUTION STATEMENT (of the abstract entered in Block 20 if different from Report)		
18. SUPPLEMENTARY NOTES		
19. KEY WORDS (Continue on reverse side if necessary and identify by block number) Test and evaluation of U.V. Fiber Optics for use as aircraft fire detectors.		
20. ABSTRACT (Continue on reverse side if necessary and identify by block number) It was found that in the U.V. solar blind region, there are severe limitations on the field of view obtainable in Fiber Optic coupled systems. These restrictions are such as to make further consideration of the wide angle system concept unprofitable. This effectively limits the use of such systems in fire detection to applications where the precise location of a flame can be predicted. It is concluded that the performance of optical fibers in the U.V. solar blind wavelengths is such that the trade-off gains proposed in AFAPL-TR-78-84 cannot be realized in practice.		

SUMMARY

This program was undertaken as a logical follow-on study of the design concepts proposed in AFAPL-TR-78-84, and with the particular aim of measuring and evaluating the performance of optical fibers in the short wavelength, U.V. solar blind region.

Specified components were obtained from commercial sources and evaluated for the properties relevant to both the design concepts of wide angle and long reach optically coupled systems.

It was found that, in the U.V. solar blind region, there are severe limitations on the field of view obtainable in fiber optic coupled systems. These restrictions are such as to make further consideration of the wide-angle system concept unprofitable, particularly against a background of changed trade-off parameters such as significant weight reduction in direct viewing sensors.

Long reach systems were modeled with a variety of input optical systems. Significant optical gains could be made, but only at the expense of further restriction on the angle of view. This effectively limits the use of such systems in fire detection to applications where the precise location of a flame can be predicted.

It is concluded that the performance of optical fibers in the U.V. solar blind wavelengths is such that the trade-off gains proposed in AFAPL-TR-78-84 cannot be realized in practice.

TABLE OF CONTENTS

<u>SECTION</u>		<u>PAGE</u>
1.	Introduction	1
2.	Theoretical Considerations	2
3.	Measurement of Fiber Properties in the U.V.	4
	3.1 Optical Fibers Tested	4
	3.2 Experimental Details	5
	3.2.1 Fiber Preparation	5
	3.2.2 Transmission Measurements	5
	3.2.3 Numerical Aperture Measurements	6
	3.3 Results	6
	3.3.1 Transmission Measurements	6
	3.3.2 Field of View Measurements	7
	3.4 Discussion	8
	3.4.1 Transmission Measurements	8
	3.4.2 Field of View Measurements	9
	3.5 Implications for Flame Detection	10
4.	Tests of a Model "Long Look" Detector System	12
	4.1 Design of System and Test Procedure	12
	4.1.1 Input System	12
	4.1.2 Tests with Gas Discharge Photocells	13
	4.2 Results	14
	4.2.1 Input System	14
	4.2.2 Results with Gas Discharge Photocells	15
	4.3 Discussion	15
5.	Summary of Test and Evaluation Results	18
6.	Conclusions	19
	References	20
	Appendix -- Manufacturers Data Sheets - Schott - ESKA - QSF	41

TABLES

Table 1	Manufacturers Information on Fiber Types Tested	21
Table 2	Transmission and Field of View of Fibers Tested	22
Table 3	System Tests with a Gas Discharge Photocell	23

TABLE OF CONTENTS

<u>SECTION</u>		<u>PAGE</u>
	<u>FIGURES</u>	
Figure 1	Optical Detectors: Field of View Against Gain	24
Figure 2	Experimental Arrangements	25
Figure 3	Transmission of Schott Fiber Bundles as a Function of Length	26
Figure 4	Field of View of Schott 2 x 500 mm Fiber Bundle at 254 nm	27
Figure 5	Field of View of Schott 2 x 500 mm Fiber Bundle at 214 nm	28
Figure 6	Field of View of Schott Fiber Bundles as a Function of Length	29
Figure 7	Input Arrangements with a 50 mm Focal Length Objective Lens	30
Figure 8	Input Arrangements with a 25 mm Focal Length Objective Lens	31
Figure 9	Optical Gain Versus Aperture Area Ratio, System 1	32
Figure 10	Optical Gain Versus Aperture Area Ratio, System 2	33
Figure 11	System Gain Against Aperture, System 1	34
Figure 12	System Gain Against Aperture, System 2	35
Figure 13	Field of View, 214 nm, System 1	36
Figure 14	Field of View, 214 nm, System 2	37
Figure 15	Field of View, 214 nm	38
Figure 16	Field of View, 214 nm, System 1	39
Figure 17	Field of View Against Gain Calculated by the Lagrange Invariant	40

1. INTRODUCTION

The Air Force has maintained a continued interest in optical methods of detecting engine nacelle fires for over 20 years. During this time there have been several developments in technology, making it possible to now provide systems with true volume coverage of a fire zone, with fast response to a hazard, while remaining unresponsive to other radiation signals present in the aircraft environment. Such systems have reached the stage of flight demonstration on high performance aircraft and are currently configured to utilize gas-discharge electron tube flame sensors for direct viewing of the potential hazard volumes. The sensors operate in the range below 280 nanometers wavelength and are not sensitive to solar radiation. It has also been realized that there may be penalties associated with the use of direct viewing sensors, including (a) the number of sensors required to "see" all parts of an obstructed volume, (b) the sensor weight, particularly when comparing early U.V. detectors with in-service thermal detection systems, and (c) the wiring required in the fire zone, with its weight and cost implications.

A potential method of reducing these penalties of direct viewing sensors is the use of fiber optic coupling from the hazard volume to a remotely located sensor. This may provide a method of both reducing the number of sensors required and eliminating aircraft wiring within the fire zone. These concepts are discussed in a study of the Applicability of Fiber Optics to Aircraft Fire Detection Systems (AFAPL-TR-78-84). The results of the study indicated the need for quantitative test data, particularly at short wavelength U.V. where there was a lack of published data. It was the objective of this follow-on program to determine the specific limitations and capabilities of current U.V. fiber optics and coupling techniques for aircraft fire detection.

The work described in this report falls into two main parts, the first concerning measurement of the transmission of U.V. radiation through commercially available optical fibers and the second, the investigation of model flame detection systems including input and output optical coupling.

The theoretical considerations, practical measurements, and applicability of results to fire detection systems are discussed.

2. THEORETICAL CONSIDERATIONS

It was shown in Reference 1 that the optical gain through a lens system between a source and a detector can be expressed as:

$$\frac{p(\lambda)_s}{p(\lambda)_b} = \left(\frac{A_s}{A_b}\right) \left(\frac{d_b}{d_s}\right)^2 T_s \quad (1)$$

where: $p(\lambda)_s$ is the power coupled to the detector (at wavelength λ) via the optical system with input aperture at distance d_s from source.

$p(\lambda)_b$ is the power coupled to a "bare detector" at a distance d_b from the source.

A_s is the effective aperture area of the optics system.

A_b is the effective sensitive area of the bare detector.

T_s is the lumped transmission coefficient of the optical system.

Therefore, comparing a bare detector and the lens system at the same distance from the source ($d_b = d_s$) the maximum possible optical gain ($T_s = 1$) is:

$$\frac{p(\lambda)_s}{p(\lambda)_b} = \frac{A_s}{A_b} = G(\lambda) \quad (2)$$

This quantity can be made very large by using large diameter input apertures. However, large apertures necessarily introduce restrictions on the field of view of the system. It can be shown that (Reference 2):

$$\frac{a \propto}{N'd} \leq 1.0 \quad (3)$$

where a = objective aperture diameter
 d = detector diameter
 N' = refractive index of medium adjacent to detector
 α = half angle of field of view.

This is a theoretical limit and its derivation makes no assumptions about the optical system between the input aperture and the detector. This system can include any type of optical component, e.g., lens, mirror and light pipes. In practice, it is difficult to design systems to approach theoretical performance, and a more realistic limit is:

$$\frac{a \alpha}{N'd} \leq 0.5 \quad (4)$$

Equations 3 or 4 can be combined with Equation 2, assuming a circular detector, to give a relationship between optical gain and maximum field of view:

$$\alpha = \frac{N}{\sqrt{G}} \quad (5a)$$

$$\text{or } \alpha = \frac{0.5 N'}{\sqrt{G}} \quad (5b)$$

Equations 5a & 5b are plotted at Figure 1 for an air immersed system ($N' = 1$). The effect of seeking large optical gain in a system is seen to be that severe limitations are placed on the field of view available.

The implication of this in a fiber optic coupled fire detection system is that optical gain may be used to compensate for transmission losses in the fiber and retain the performance of a bare detector in terms of sensitivity, but only at the expense of severe restriction of the field of view.

3. MEASUREMENT OF FIBER PROPERTIES IN THE U.V.

It was recognized in the previous study (AFAPL-TR-78-84) that inadequate data was available on optical fibers in the U.V. solar blind region, and that quantitative information should be acquired before design concepts could be pursued.

A prime task of this program was to develop the required data, and that work is recorded in this section of the report. The fiber samples were obtained from commercial sources and performance data developed in the U.V. short wavelength region, with particular emphasis on the measurement of Transmission and Numerical Aperture, key factors in determining the potential application to fire detection systems.

3.1 Optical Fibers Tested

- 1) Silicone coated silica fibers manufactured by Jena Glasswork Schott and Gen. (obtained from Schott Glass Ltd., Drummond Road, Stafford ST16 3EL, U.K.). These fibers were made up into fiber bundles with protective metal or plastic sheathing.

- 2) Silicone coated silica fiber manufactured by Quarts et Silice (obtained from Nuclear and Silica Products Ltd., 44-46 The Green, Wooburn Green, High Wycombe, Bucks, HP10 OEU, U.K.). This was in the form of a single fiber type QSF 300 with a protective Tefzel coating.

- 3) ESKA acrylic optical fiber manufactured by Mitsubishi Rayon (obtained from Optronics Ltd., Cambridge Science Park, Milton Road, Cambridge, CB4 4BH, U.K.). This was in the form of a single fiber with a protective coating.

A summary of the manufacturers data on these fibers is given in Table 1.

3.2 Experimental Details

3.2.1 Fiber Preparation

Fiber bundles of type 1 required no preparation as they were supplied with finished ends and end fittings in three different lengths. However, fibers of types 2 and 3 were supplied as sample lengths with no end preparation. They were therefore cut to suitable lengths and the ends mounted in an epoxy resin and the cut surfaces polished flat with diamond grit to reduce scattering losses at the input and output. The quality of the polishing was tested by measuring transmission through the fiber with visible radiation.

3.2.2 Transmission Measurements

Transmission measurements were made in the U.V. at two discrete wavelengths, 254 nm and 214 nm. These wavelengths were chosen as they fall within the bandwidth (200-260nm) of gas discharge tube detectors currently in use as solar blind flame detectors. The source for the 254 nm measurements was a mercury discharge lamp (Philips Type 0Z4W), used with a narrow band filter to select the 254 nm U.V. emission line. The source for the 214 nm measurements was a zinc hollow cathode lamp, again used with a narrow band filter to select the 214 nm emission line. The experimental arrangement used for the transmission measurements is shown in Figure 2 (a). The input numerical aperture for the system was very small ($\alpha < 1$ degree) so that the transmission measured was essentially for parallel illumination perpendicular to the end of the fiber. Measurements were taken of the input intensity of illumination by placing the detector behind the input aperture. The overall transmission coefficient was then obtained by measuring the intensity of radiation at the end of the fiber. The attenuation of the fiber, as a function of length, was investigated by measuring the transmission for different lengths of each fiber and assuming that the input and output losses were constant. The detector normally

3.2.2 (Continued)

used was a photomultiplier tube with a U.V. extended sensitivity photocathode (EMI Type 6256S). Some measurements were also made with U.V. extended silicon photodiodes (RCA C30843; E.G. & G. 444B; Centronics OSD 100-1). These measurements were, however, less satisfactory, as the output from these detectors was always due in part to the visible radiation produced by the sources, even with the narrow band filters present, so readings of U.V. intensity were made by inserting a glass plate into the input beam, which removed the U.V. radiation, and recording the change in output signal of the detector. This procedure was not necessary with the PMT, as the output signal due to the visible radiation present was not significant. Measurements were also made using an unfiltered tungsten lamp as source and a silicon photodiode as the detector as a check on the experimental conditions. These measurements are for a band of wavelengths in the visible and near infrared, probably biased to $\sim 0.9 \mu\text{m}$ because of the lamp output and detector sensitivity peaking in this region.

3.2.3 Numerical Aperture Measurements

The field of view of the optical fibers was measured with the source arrangement shown in Figure 2(a) except that the input end of the fiber was mounted on a rotation table and the input aperture was removed, shown schematically in Figure 2(b). Measurements of the transmitted radiation were recorded as a function of the angle between the direction to the source and the normal to the fiber end. Measurements were made at the same wavelengths as the transmission measurements, 214 and 254 nm, and with the broad band visible/I.R. system.

3.3 Results

3.3.1 Transmission Measurements

The measured transmission values for the fibers tested are summarized

3.3.1 (Continued)

in Table 2. No transmission in the U.V. could be measured for the ESKA plastic fiber. The Quartz et Silice P.C.S. (plastic coated silica) fiber had measurable transmission at 254 nm (30%) but no transmission could be detected at 214 nm. The Schott fibers, however, had appreciable transmission at 254 nm ($> 40\%$) and at 214 nm ($> 10\%$). The error values given for the transmission measurements in Table 2 are the standard deviations in the values obtained with different detectors. The transmission values for the different Schott fiber bundles have been plotted in Figure 3 as $\ln(T/100)$ against fiber length.

A measurement of transmission at 214 nm, as a function of temperature, was also taken, using the 2 mm diameter, 255 mm long Schott fiber bundle. The central 170 mm of the fiber was heated in a tube furnace and measurements taken from room temperature (23°C) to 120°C , the maximum temperature specified for this type of fiber in the cladding as supplied. No significant difference in transmitted intensity was detected over this temperature range.

3.3.2 Field of View Measurements

Typical field of view measurements are shown in Figure 4 and 5 for the Schott 2 mm diameter, 500 mm long fiber bundle. Figure 4 shows the output signal plotted as a function of angle of rotation of the input end of the fiber with respect to the source direction for 254 nm wavelength radiation. Figure 5 shows a similar plot obtained with 214 nm radiation. From these curves the field of view has been measured as the full width at half maximum ($2\alpha_{0.5}$) and the full width at 10% of maximum ($2\alpha_{0.1}$), and these values are listed in Table 2. The collected results for the Schott fiber bundles are plotted as a function of fiber length in Figure 6. These results were all obtained using the photomultiplier tube as the radiation detector.

3.4 Discussion

3.4.1 Transmission Measurements

The transmission results shown in Table 2 indicate that of the fibers tested, only the Schott fibers had useful transmission throughout the band useful for solar blind flame detection. The Quartz et Silice fiber had some transmission at 250 nm, more than expected from the manufacturer's data (shown in Appendix A of Reference 1), but the lack of transmission at 214 nm agrees with the steeply rising attenuation through the U.V. shown in the manufacturer's data. The disagreement in absolute transmission values is not unexpected as the manufacturer's values are for long length measurements (> 250 m). Over the much shorter lengths tested here, likely to be typical of fire detection installations, higher transmissions would be expected.

The Schott results agree well with the manufacturer's transmission values for comparable lengths at 250 nm, the shortest wavelength the manufacturer provides data for. From Table 2 and Figure 3 it can be seen that there is a marked increase in attenuation from 254 nm to 214 nm, although there is still some transmission at the shorter wavelength. At shorter wavelengths the transmission values become more dependent on length and more variable between individual samples. The length dependence should be due, at least in part, to the increasing attenuation of the radiation in the silica core. From Figure 3 the attenuation coefficients can be estimated using:

$$I = I_0 \exp(-\beta L)$$

where

I = transmitted intensity
 I_0 = input intensity
 L = length of fiber
 β = absorption coefficient

$$\ln \frac{I}{I_0} = \ln \frac{T}{100} = -\beta L$$

The difference in the value of β at different lengths is estimated in order to eliminate end effects.

3.4.1 (Continued)

This gives values for β of $\leq 0.3 \text{ m}^{-1}$ at 254 nm and of 0.4 - 1.2 m^{-1} at 214 nm. The higher values are probably more reliable as these are consistent with the measurements from the two fibers which are more similar in the visible/IR measurements.

The difference in transmission between individual fiber bundles is contributed to by variations in input and output efficiencies (reflectance losses), scattering due to faults or impurities in the fibers and possibly changes in refractive index of the cladding material. All of those effects might be expected to become more important in the U.V. causing the variation between samples to increase. Included in the transmission losses at all wavelengths is the absence of fibers over some of the input area due to the packing fraction and the loss of some individual fibers due to breakage.

3.4.2 Field of View Measurements

The results show that the field of view, or the input numerical aperture of a fiber in the U.V., is very restricted. The field of view for a fiber is determined by the refractive indices of the core and cladding materials:

$$\text{N.A.} = n_0 \sin \alpha = (n_1^2 - n_2^2)^{1/2}$$

where

N.A. = numerical aperture.

n_0 = refractive index of ambient

n_1 = " " " core

n_2 = " " " cladding

n_1 and n_2 are functions of wavelength and tend to become closer together at shorter wavelengths; therefore, the field of view progressively reduces for shorter wavelength radiation as demonstrated by Figure 6. This obviously restricts the area a fiber alone could survey but it also places restrictions on any optical system designed to collect radiation to increase

3.4.2 (Continued)

the transmitted signal through a fiber optic to a radiation detector. There is also a tendency for the field of view to decrease with fiber length, due to higher attenuation for rays with higher input angle, and there is some suggestion of this tendency in Figure 6.

3.5 Implications for Flame Detection

For a flame detection system, considering a detector sensitive in the band 200-250 nm, collecting all the radiation output from an optical fiber 1 m long, the transmission possible with Schott fibers would be of the order of 25%. Thus, if there were no input optics to the fiber, and the fiber area is the same as the detector sensitive area, the effective sensitivity in the fire zone would be only 25% that of a bare photocell at the same temperature conditions. The use of fiber optic coupling does enable the removal of the detector to a lower temperature environment, but the loss of sensitivity with temperature of the detector is not large. Typical sensitivity at 260 °C is still greater than 70% of that at 20 °C. It is seen also that the 25% transmission through the fiber is only operative over a small angular field of view of approximately ± 5 degrees. Thus it would require many fibers feeding into the same photocell to cover the same field as a bare photocell (typically ± 45 degrees). To increase the sensitivity, either the fiber optic area could be increased or an input lens system of larger aperture than the fiber could be used. In both cases, however, the field of view would necessarily be restricted according to Equation 3 and Figure 1. In the first case, there would have to be an optical system transferring the radiation from the fiber output to the detector for good transfer efficiency, and this would be difficult and complicated to arrange for many fibers feeding into the same detector. In the second case, it would be difficult to increase the field of view over that of a bare fiber and increase the input signal simultaneously, even to the limit of Equation 3, as the numerical aperture of the fiber puts severe constraints on the design of the

3.5 (Continued)

optical system. Thus, it would appear unprofitable to pursue the "wide angle" design concept, as the system would become necessarily complex to match the performance of a bare photocell in terms of sensitivity and field of view. Additionally, it is noted that other programs supported by AFAPL, particularly the development of a U.V. Advanced Fire Detection System, have significantly altered the trade-off data. Bare detector weight is now realistically 0.12 lb. compared with over 7 lbs. premised in the previous study (Reference 1).

It does seem possible, however, to design an input system which has higher sensitivity along any one given direction, the "long reach" system discussed in Reference 1. This system would have to have a gain of at least four times to overcome losses in the fiber (or at least three times, allowing for loss of cell sensitivity at fire zone temperatures up to 260 °C), but much larger gains than this are theoretically possible according to Equation 2. The construction and testing of a model system is described in the following section.

4. TESTS OF A MODEL LONG REACH DETECTOR SYSTEM

4.1 Design of System and Test Procedure

4.1.1 Input System

The input system used for significant optical gains must collect radiation over a relatively wide aperture with respect to the fiber aperture and channel this radiation into the fiber over a small numerical aperture. The simplest possible input system would be a single converging lens focusing radiation from a distant source onto the front end, but the numerical aperture of the fiber limits the aperture available, as shown schematically in Figures 7(a) and 8(a) for lenses of focal lengths 50 mm and 25 mm, respectively. The obvious way to improve this situation is to use a second diverging lens close to the focus of the first lens to reduce the angle at which the light is fed into the fiber. The improvements in available aperture expected using a 2 mm diameter fiber bundle for a 50 mm focal length lens combined with a -4 mm focal length lens is shown in Figure 7(b). This combination of lenses is referred to as System 1 below. A similar diagram for a 25 mm focal length and a -4 mm focal length lens, referred to as System 2, is shown in Figure 8(b). The properties of these four arrangements were investigated using synthetic silica lenses with high transmission down to 200 nm and 2 mm diameter Schott fiber bundles of length 500 and 1000 mm.

The input systems were tested initially for "optical gain" by measuring the ratio of outputs of the optical fiber with the PMT with and without the optical system at the input. The source used for all the tests was the zinc hollow cathode lamp producing radiation of 214 nm wavelength at 600 mm from the input aperture. The optical system under test was adjusted to give maximum output for this source distance.

4.1.1 (Continued)

The "system gain" was then determined by measuring the intensity of radiation at the input position using the PMT directly. The measurements were carried out for a range of input apertures by placing a variable aperture in front of the objective lens. Field of view measurements were also taken for each system by rotating the system about a vertical axis through the objective lens and measuring the output as a function of the angle of rotation.

4.1.2 Tests with Gas Discharge Photocells

The only types of photocell currently in use as a flame detector in aircraft are gas discharge photocells. These photocells present some problems with regard to collecting the radiation from the optical fiber output as the sensitive area of the photocathode is relatively small in one dimension, non-circularly symmetric and at the center of a glass envelope so that fiber ends cannot be placed close to the cathode. Thus, for some of the tests using this type of photocell as the detector, a short focal length lens was interposed between the fiber output and the detector in order that a demagnified image of the fiber output was produced at the detector cathode. The detector used throughout the tests was a Graviner D6100 photocell in which the cathode is 0.5 mm diameter wire approximately 7 mm long. The sensitive area of the photocell is smaller than this in individual photocells by a variable amount difficult to determine. The tests were conducted by measuring the count rate of the photocell at the input position and then measuring the count rate with the photocell at the output position of the system under test. The signal strength measured at the two positions was compared by correcting the measured count rates to the equivalent count rate at zero dead time in the associated operating circuit. The results are therefore quoted as the signal strength as a percentage of the bare photocell value. The source for all the tests was the zinc hollow cathode lamp at 60 cm from the input to the system.

4.2 Results

4.2.1 Input System

The best optical gains obtained with the 50 mm focal length lens alone and with input system 1 are plotted as a function of A^2/D^2 where:

A = objective aperture diameter

D = fiber bundle diameter = 2 mm

in figure 9. A similar plot for the 25 mm focal length lens and input system 2 is shown in Figure 10. For zero losses in the input lenses these curves should follow a straight line of gradient 1 and this is approached for the single lenses at small apertures. However, the limitation of the useful aperture due to the small numerical aperture of the optical fibers is readily apparent. There is obviously an improvement in the useful aperture introducing the second lens into the input system, but there are more losses introduced into the system as evidenced by the lower gradient of the straight line proportion of the curves for system 1 and system 2. This means that higher gains are obtained with a single lens at small apertures but that higher gains can be obtained with the two lens systems at larger apertures, although the useful aperture limit on system 2 at 12 mm diameter is obvious, and even system 1 becomes progressively less efficient at large apertures.

Similar results to those shown in Figures 9 and 10 are shown in Figures 11 and 12 for the different input systems, however, plotting system gain, i.e., including losses in fiber transmission, directly against objective aperture diameter.

The fields of view of the four input systems are shown in Figures 13 and 14. These are very restricted in all cases but the addition of the second lens caused a marked reduction of the field of view of both system 1 and system 2.

4.2.2 Results with Gas Discharge Photocells

Results obtained using gas discharge photocells as the radiation detector are shown summarized in Table 3 for line of sight measurements. These results show the same pattern as those obtained with the PMT, the largest signal levels being obtained with the input system 1. The addition of the lens between the output of the fiber and the photocell improved the signal by a factor of between 2 and 4, depending on the input conditions, the greater improvement being obtained when the input numerical apertures of the fibers were completely filled as in arrangement 8.

The field of view of a fiber bundle alone coupled to a gas discharge photocell by a 10 mm focal length lens is shown in Figure 15. The field of view is similar to, but slightly less than the same fiber bundle with the PMT as the detector. Figure 16 shows the field of view obtained with arrangement 6 from Table 3. In this case, the field is narrower than that obtained with the PMT.

4.3 Discussion

The results obtained with the various input systems show that significant optical gains can be obtained along a particular line of sight, but only at the expense of extremely limited fields of view. Fields of view are somewhat improved with shorter focal length lenses, but in this case it becomes more difficult to use large apertures and thus obtain high gains. This effect can be quantified by considering the optical input system as producing an image of the field of view at the optical fiber input and applying the Lagrange Invariant (see for example Reference 3) at the object and image. The Lagrange Invariant, I , is constant for any optical system and is defined by:

4.3 (Continued)

where $I = hnu = h'n'u'$
 h, h' are the heights of the object and image
 n, n' are the refractive indices of the mediums that
the object and image are immersed in
 u, u' are the angles that rays at the base of the
object and image make with the optic axis.

Clearly, at the input to a fiber, h' cannot be greater than the radius of the input area and u' cannot be greater than π or light from the object is not transferred into the fiber. Therefore, for a given fiber there are restrictions on the possible values of I and therefore on the possible optical systems that are able to transfer radiation to the fiber from the object.

In particular, if we consider the experimental conditions used above of a Schott 2X 1000 mm fiber bundle with a source of 214 nm wavelength at 600 mm from the input aperture.

$I \leq 1 \times 1 \times 3.7$ mm degrees
at the image.

Therefore at the object

$h u \leq 3.7$ mm degrees.

i.e., if h is large, u must be small and vice versa. h defines the field of view and u defines the useful aperture at the objective lens. Thus, this relationship can be converted to a graph of field of view against available optical gain, and this has been done in Figure 16. This graph has the same form as the general restriction on any optical detector shown in Figure 1 but produces much more severe restrictions. The experimental values obtained are also plotted on Figure 17 and show that the performance obtained is approaching the limiting values, particularly at smaller apertures. At larger apertures the efficiency of collection of radiation is lower, as demonstrated by Figures 9 and 10.

4.3 (Continued)

Obviously, any increase in available numerical aperture in the U.V. would be very valuable in terms of increasing the available optical gain and/or field of view. However, as observed in Paragraph 3.4.2, such increases are more difficult to achieve in the U.V. than at longer wavelengths.

The severe restrictions on the field of view and gain produced by currently available fiber optics mean that, for conventional fire detection systems, any line of sight gain is of little value. Gains in signal level are only obtained for point sources whereas most fires are extended sources and only a small part will be on the line of sight of the detector. For example, a 5 inch panfire at 4 feet occupies an angular field of view of approximately ± 3 degrees, and a detector with a field of view (α) of 0.6 degrees would only respond to radiation from 4 percent of its area. Thus, a line of sight system gain of 25 would be required in order to produce the same signal level as a bare detector at the same temperature conditions. Allowing for a loss of sensitivity of less than 30 percent for the bare detector if operated at temperatures up to 260 °C, then the required gain is modified to about 18 to achieve the same signal level.

Nevertheless, there may be situations where the narrow field of view is relatively unimportant compared to, for example, the necessity of "piping" radiation from inaccessible volumes, such as wing dry bays of aircraft, provided the source intensity is sufficiently high. The practical application of fiber optic coupled fire detection systems appears to be limited to such situations.

5. SUMMARY OF TEST AND EVALUATION RESULTS

- 5.1 Currently available silicone coated silica optical fibers have useful transmissions ($\sim 25\%$) in the U.V. wavelength range of interest in fire detection over lengths of the order of 1 meter.
- 5.2 The numerical aperture of these fibers is small (approximately 0.07), however, and this places severe restrictions on the field of view available.
- 5.3 Line of sight optical gains of the order of 25 have been obtained with model input lens systems but with very restricted field of view (approximately 0.5 degrees).
- 5.4 Larger field of view can only be obtained with similar gains if optical fibers become available with higher numerical apertures in the U.V. This would require new cladding materials that maintain a higher refractive index difference between cladding and core into the U.V. wavelengths. However, very large improvements would be required, and there is presently no indication that such improvements could be obtained easily.

6. CONCLUSIONS

The over-riding conclusion from this program is that the field of view obtainable through fiber optic coupled systems in the U.V. solar blind region is much more restricted than had been assumed during the conceptual study recorded in AFAPL-TR-78-84.

Specified components were obtained and evaluated in the U.V. solar blind region for the optical properties essential in both the wide angle and long reach systems. Severe limitations were found in the field of view obtainable at short wavelengths which made further consideration of the wide angle concept unprofitable.

The best sample of optical fiber was tested to an environmental temperature of 120°C and showed no change of performance. The environmental performance of optical fibers is likely to be governed by the cladding materials rather than any inherent limitation of the core material.

Long reach systems were modeled with a variety of input optical systems. Evaluation showed that significant optical gains could be made at the input system but only at the expense of further severe restriction on the angle of view. This effectively limits the use of such systems as flame detectors to applications where either the precise location of a flame can be predicted or where the fire event is so widespread as to provide a large probability of radiation along a narrow line of sight.

TABLE 1

MANUFACTURERS INFORMATION ON FIBER TYPES TESTED

<u>FIBER TYPE AND CONSTRUCTION</u>	<u>TRANSMISSION</u> % 1000mm length	<u>NUMERICAL APERTURE</u>	<u>WAVELENGTH NANOMETER</u>	<u>TEMPERATURE RANGE</u>
Schott. Silicone coated silica 100 um fibers made up into bundles 2 and 3mm dia.))))	43 52 55 n/a	n/a 0.26 0.35 0.42	250 366 540 860	-40 to +120°C as sheathed
Quartz et Silice QSF 300 Silicone coated silica)) 300um single fiber, Tefzel coated))	70 ~1	 0.27	500 Not specified 250	-50 to +250°C
ESKA Polymethylmethacrylate)) coated with fluorocarbon) 1 mm. dia single fiber.)	~50	0.5	400 Not specified	-30 to +80°C

TABLE 2

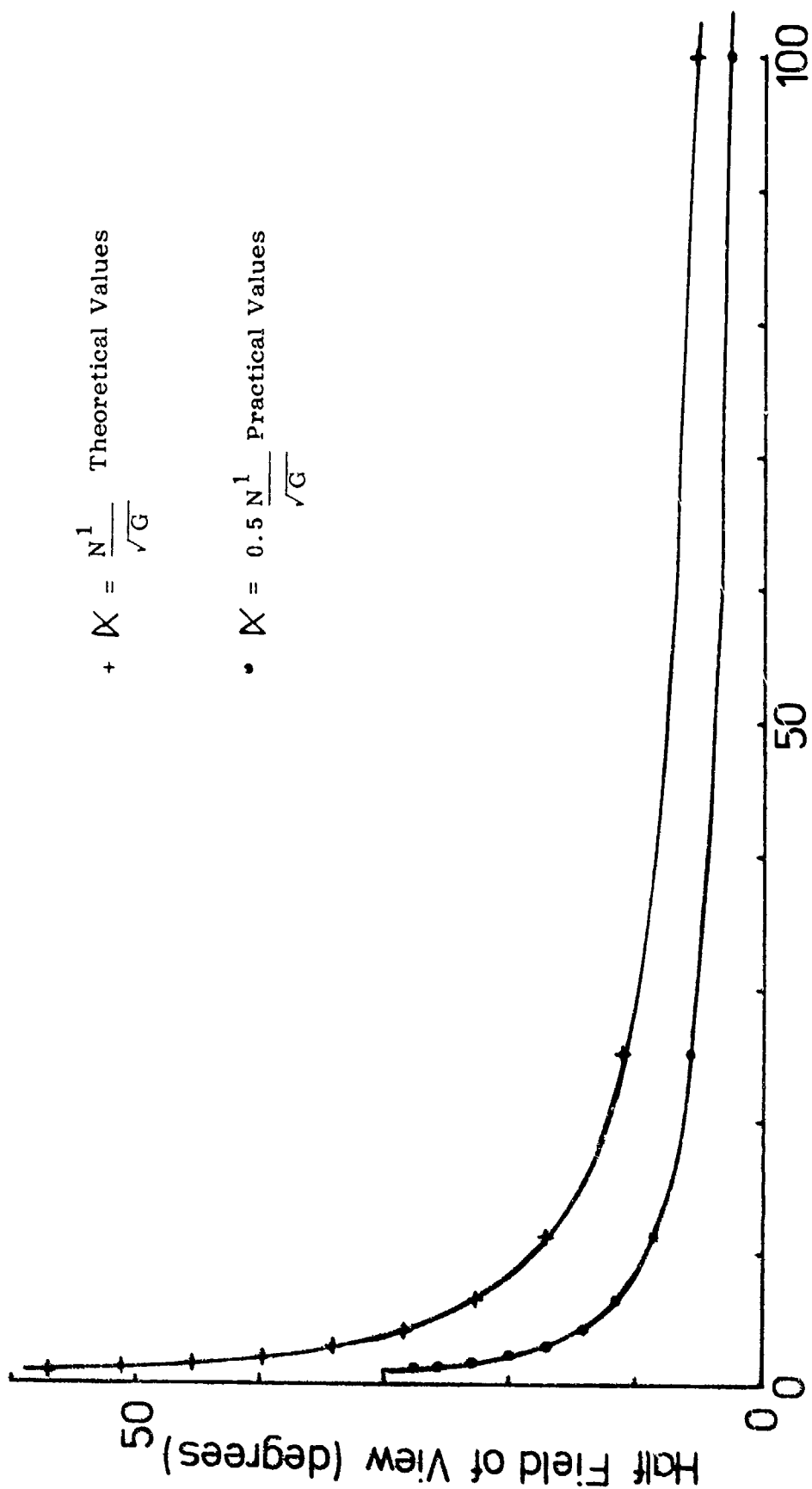
TRANSMISSION AND FIELD OF VIEW OF FIBERS TESTED

<u>Fiber</u>	<u>Diameter/Length</u> (mm)	<u>Transmission</u> %	<u>Wavelength</u> <u>Nanometer</u>	<u>2α_{0.5}</u> <u>degrees</u>	<u>2α_{0.1}</u> <u>degrees</u>	<u>Numerical</u> <u>Aperture</u>
ESKA (plastic)	1/330 (single fiber)	38	Vis.	44	54	0.37
		<0.02	254			
		<0.02	214			
Quartz et silice (PCS)	0.3/775 (single fiber)	70	Vis.	10	18	0.09
		30	254	8	16	
		<0.3	214			
Schott (PCS)	2/1600 (2mm dia. bundle of 100um fibers)	66	Vis.	41	66	0.35
		43 \pm 1	254	9.0	16.4	
		11.5 \pm 3.0	214	7.4	12.0	
"	2/500 (2mm bundle)	64	Vis.	38	59	0.325
		41 \pm 1	254	10.4	16.6	
		14 \pm 2	214	8.4	13.4	
"	2/255 (2mm bundle)	66	Vis.	40	68	0.34
		54 \pm 3	254	9.6	16.0	
		28 \pm 10	214	7.2	12.1	
"	3/255 (3mm dia. bundle of 100um fibers)	53	Vis.	52	68	0.44
		40 \pm 3	254	11.4	18.2	
		15 \pm 7	214	9.5	15.1	

TABLE 3

SYSTEM TESTS WITH A GAS DISCHARGE PHOTOCELL

	<u>Input</u>	<u>System</u> <u>Fiber</u>	<u>Output</u>	<u>Sensitivity</u> <u>% of Base Photocell</u>
1.	None	Schott 1000 x 2	None	2-3
2.	None	Schott 1000 x 2	F = 10mm lens	4-6
3.	System 2 9.5mm dia. aperture	Schott 1000 x 2	None	20±2
4.	"	" "	F = 10mm lens	60±12
5.	System 1 20mm dia. aperture	" "	None	56
6.	"	" "	F = 10mm lens	180±12
7.	F = 50mm lens 20mm dia. aperture	" "	None	17
8.	"	" "	F = 10mm lens	71

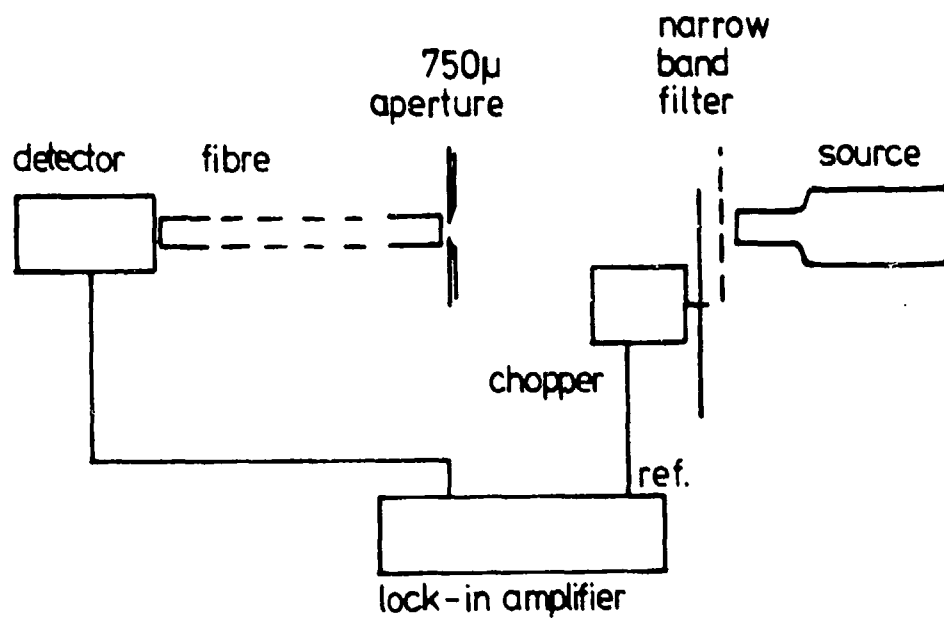


+ $X = \frac{N^1}{\sqrt{G}}$ Theoretical Values

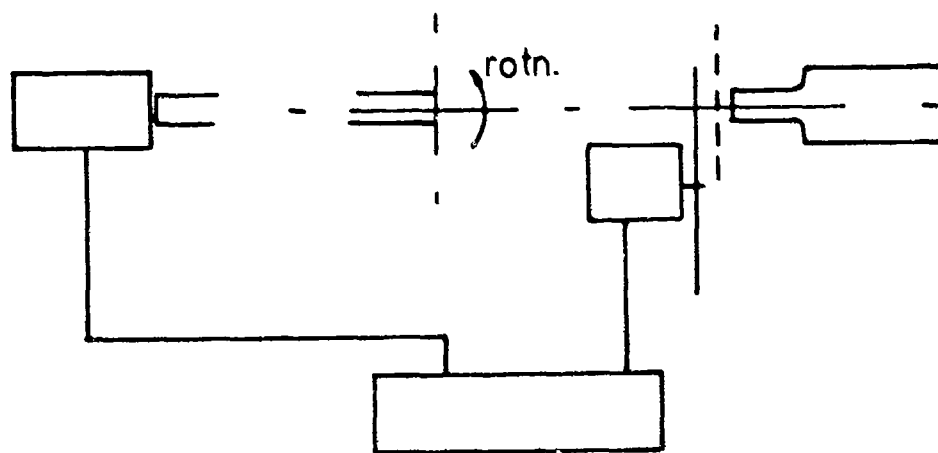
• $X = 0.5 \frac{N^1}{\sqrt{G}}$ Practical Values

Max. Optical Gain $G = A^2 / D^2$

FIGURE 1 OPTICAL DETECTORS: FIELD OF VIEW AGAINST GAIN



a). Transmission measurements.



b). Field of view measurements.

FIGURE 2 Experimental arrangements.

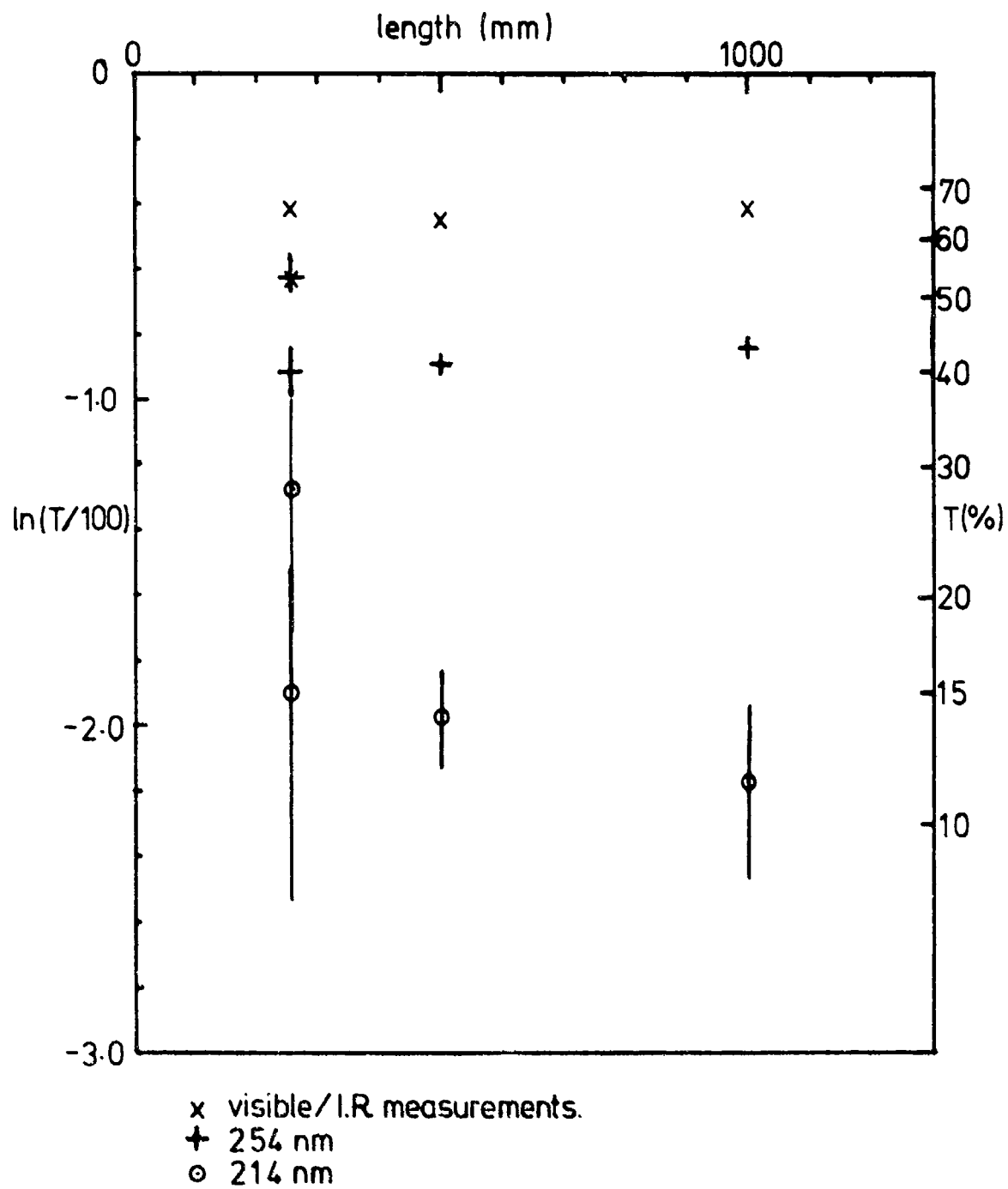


FIGURE 3

Transmission of Schott fibre bundles as a function of length.

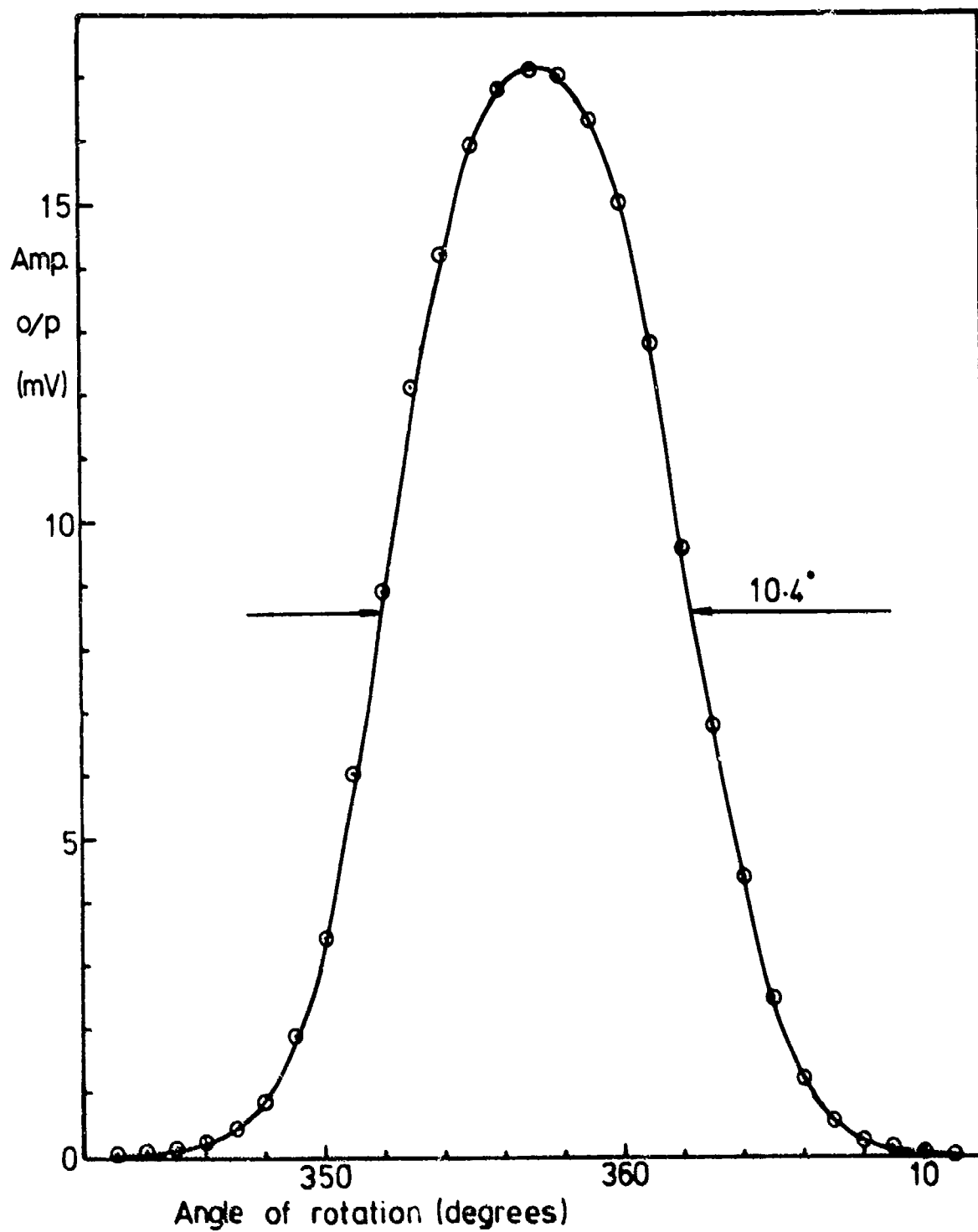


FIGURE 4 Field of view of Schott 2x500 mm fibre bundle at 254 nm.

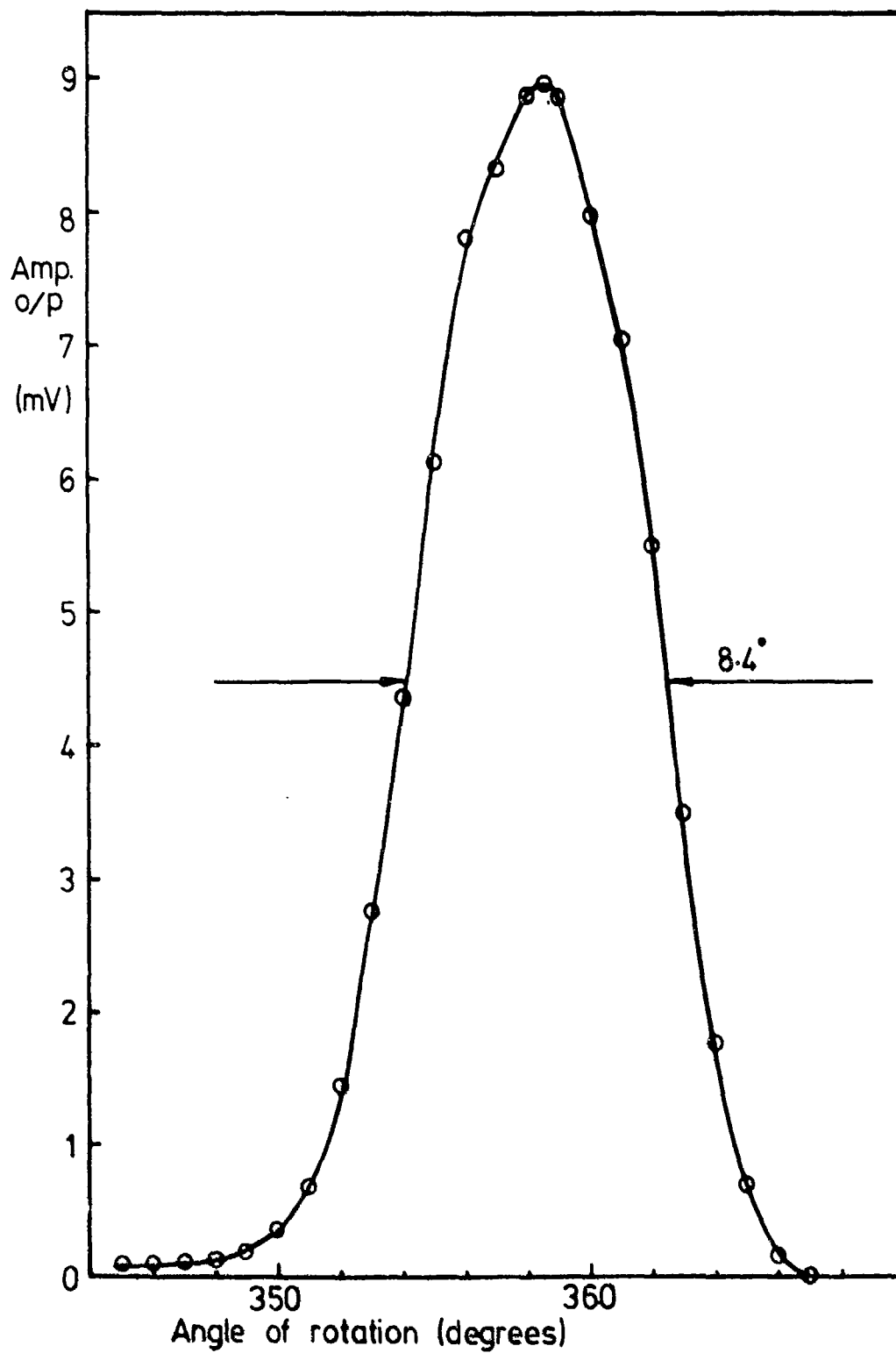


FIGURE 5 Field of view of Schott 2x500mm fibre bundle at 214nm

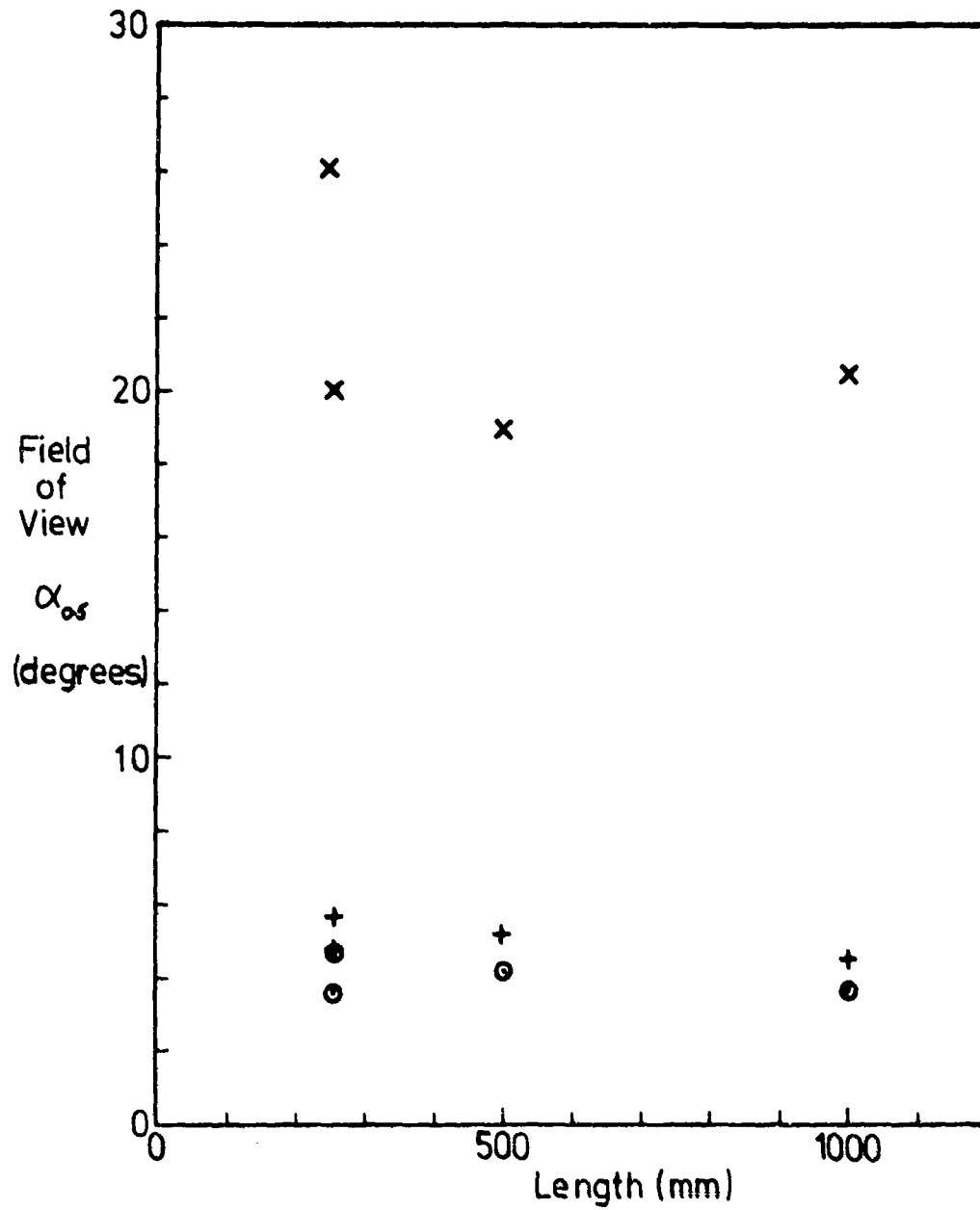
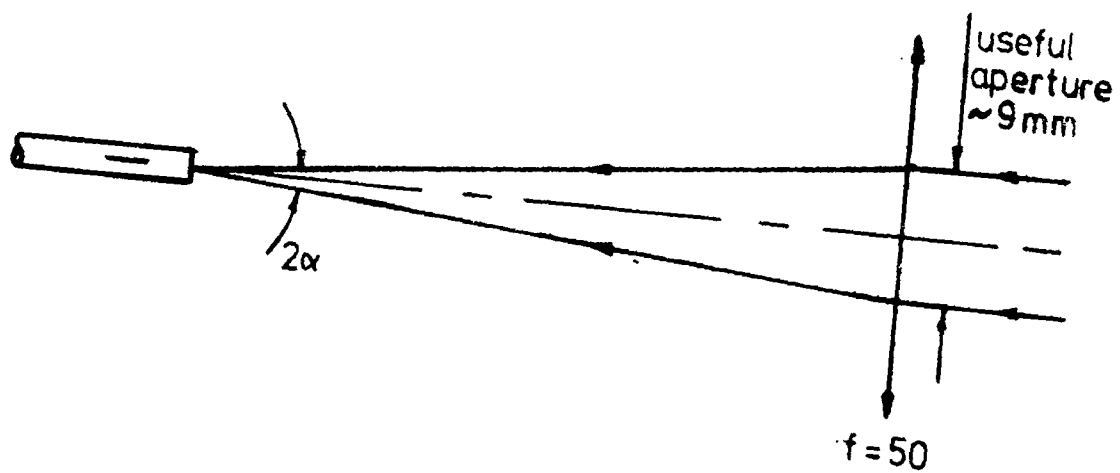


FIGURE 6 Field of view of Schott fibre bundles as a function of length.
 x Visible/I.R. measurements
 + 254 nm
 o 214 nm

a). Objective lens only



b). Input system 1

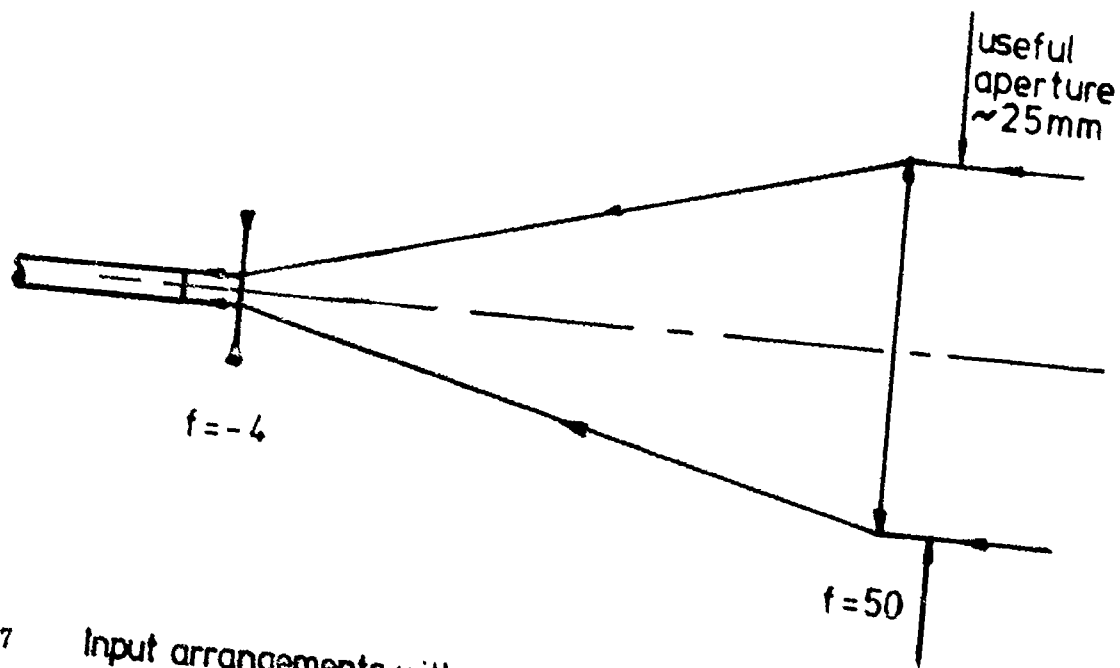
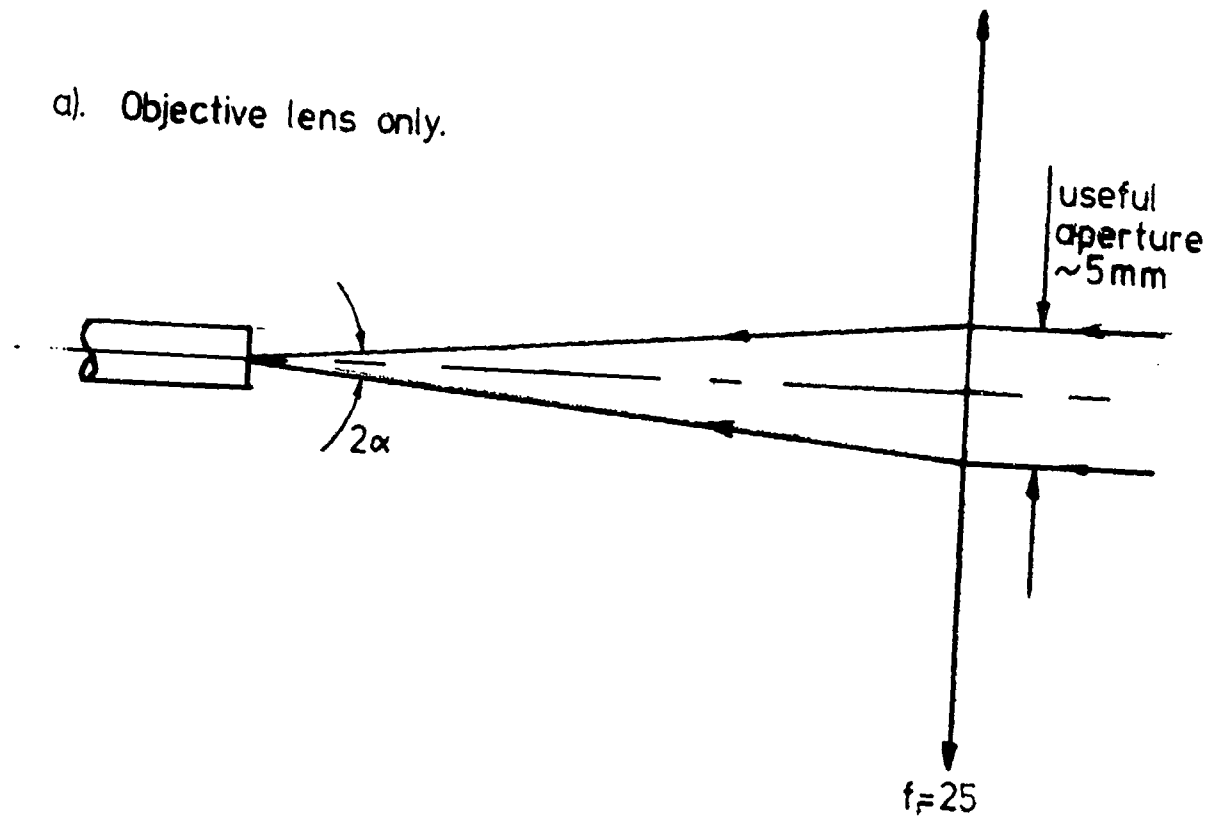


FIGURE 7 Input arrangements with a 50mm focal length objective lens.

a). Objective lens only.



b). Input system 2

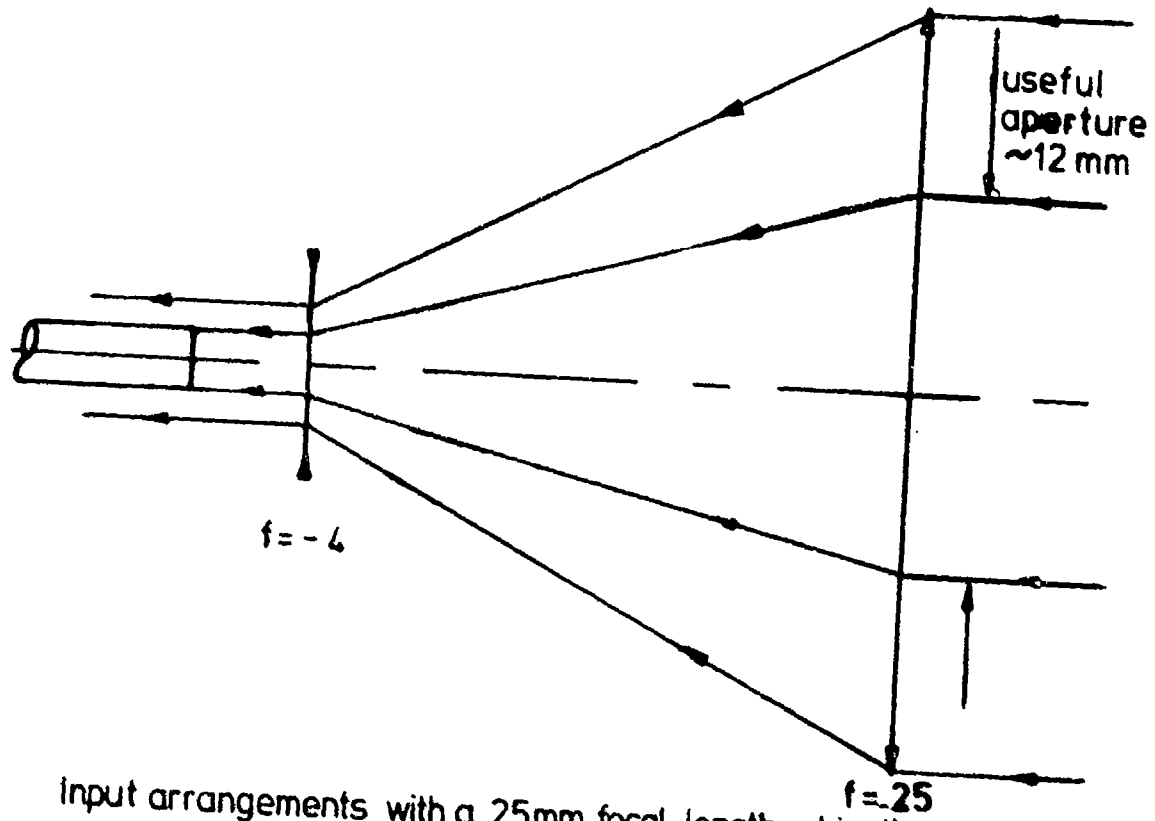


FIGURE 8 Input arrangements with a 25mm focal length objective lens.

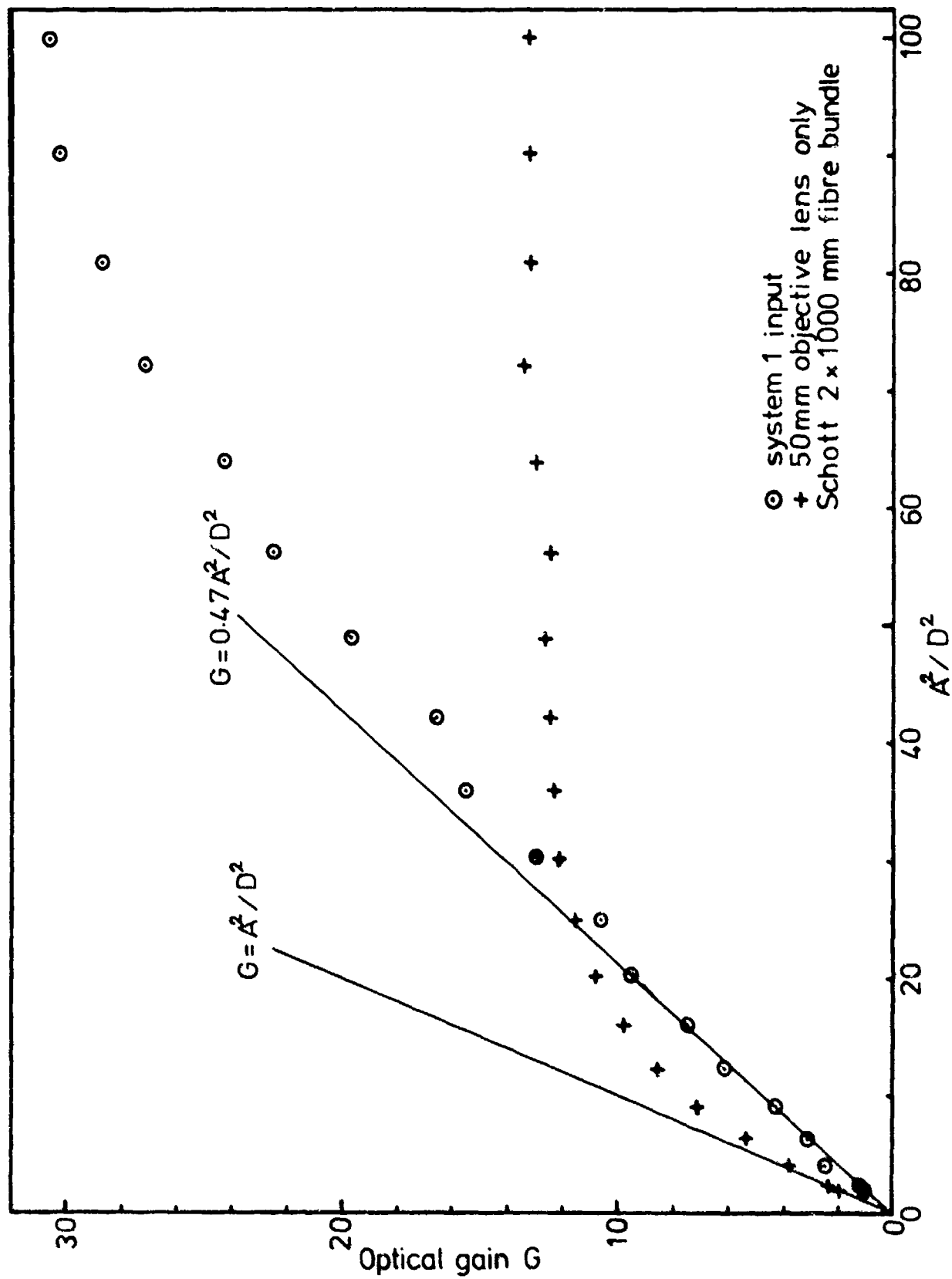
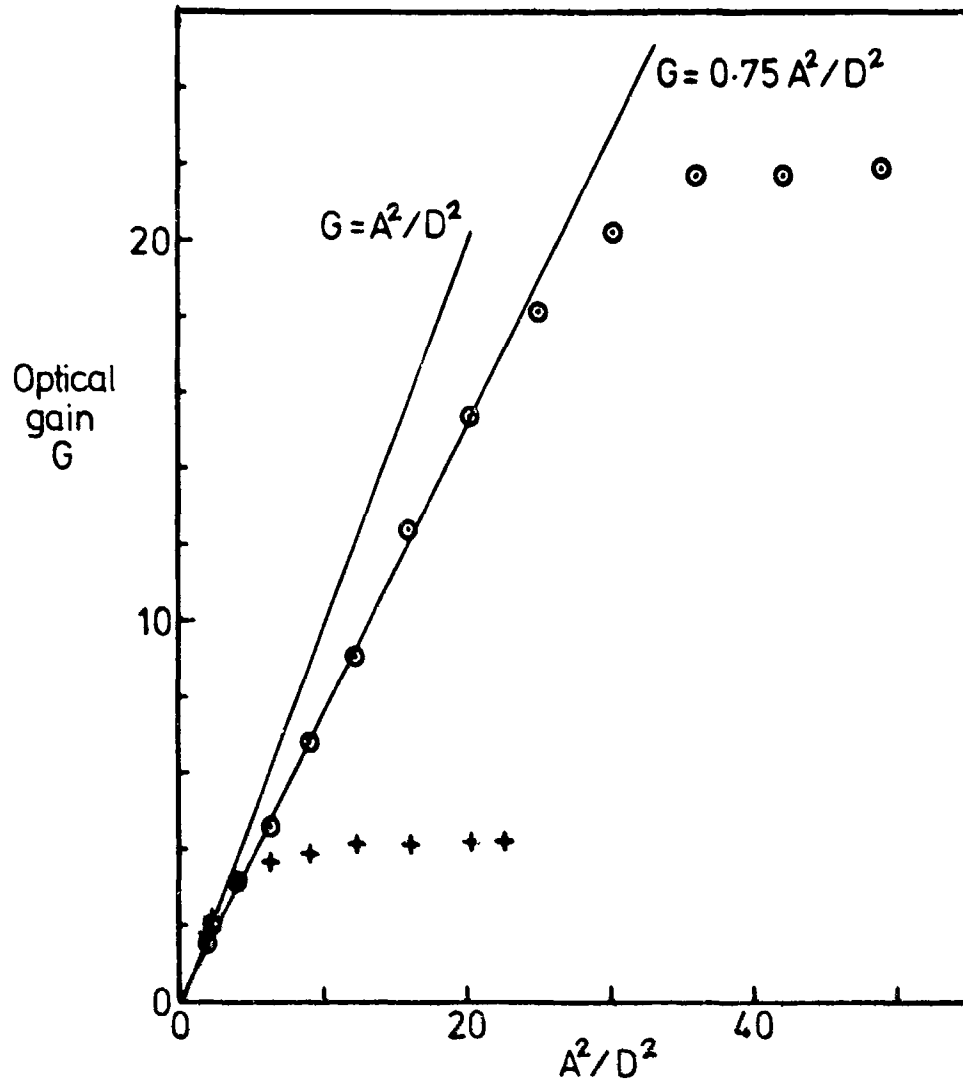


FIGURE 9 OPTICAL GAIN VERSUS APERTURE AREA RATIO



⊙ system 2 input
 + 25mm objective lens only
 Schott 2×500 mm fibre bundle

FIGURE 10 Optical gain versus aperture area ratio

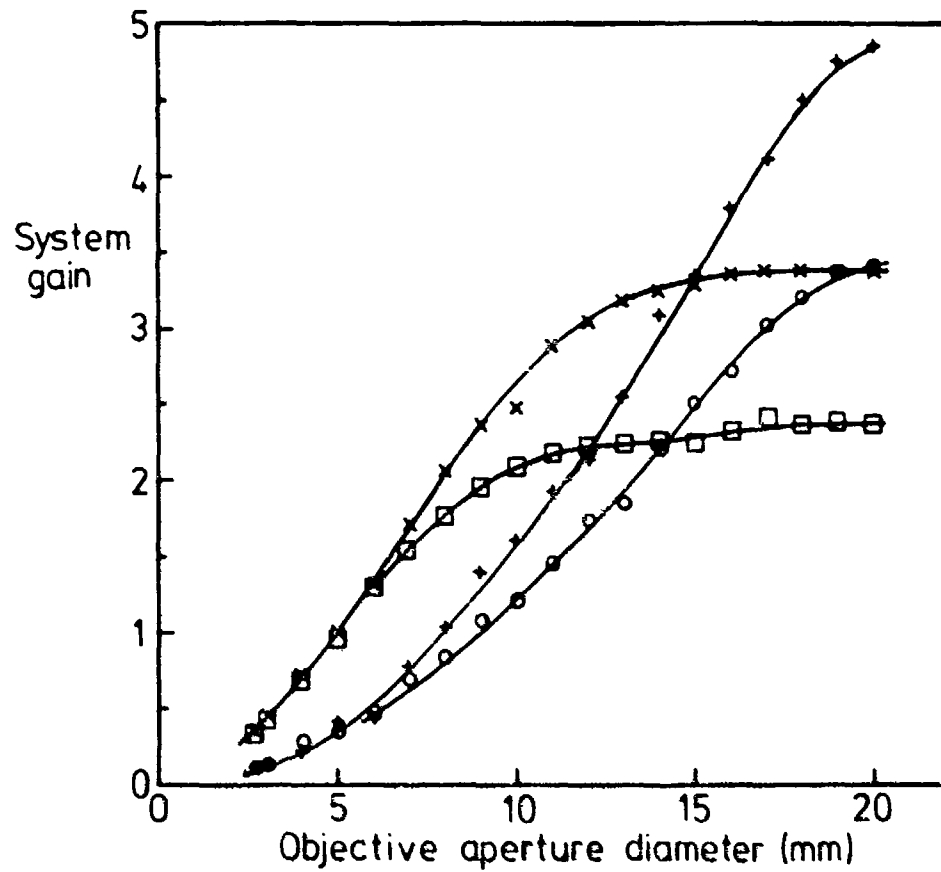


FIGURE 11 System gain against aperture
 o 2x1000mm Schott fibre bundle, system 1
 + 2x 500 " " " " " "
 □ 2x1000 " " " " .50mm lens only
 x 2x 500 " " " " " "

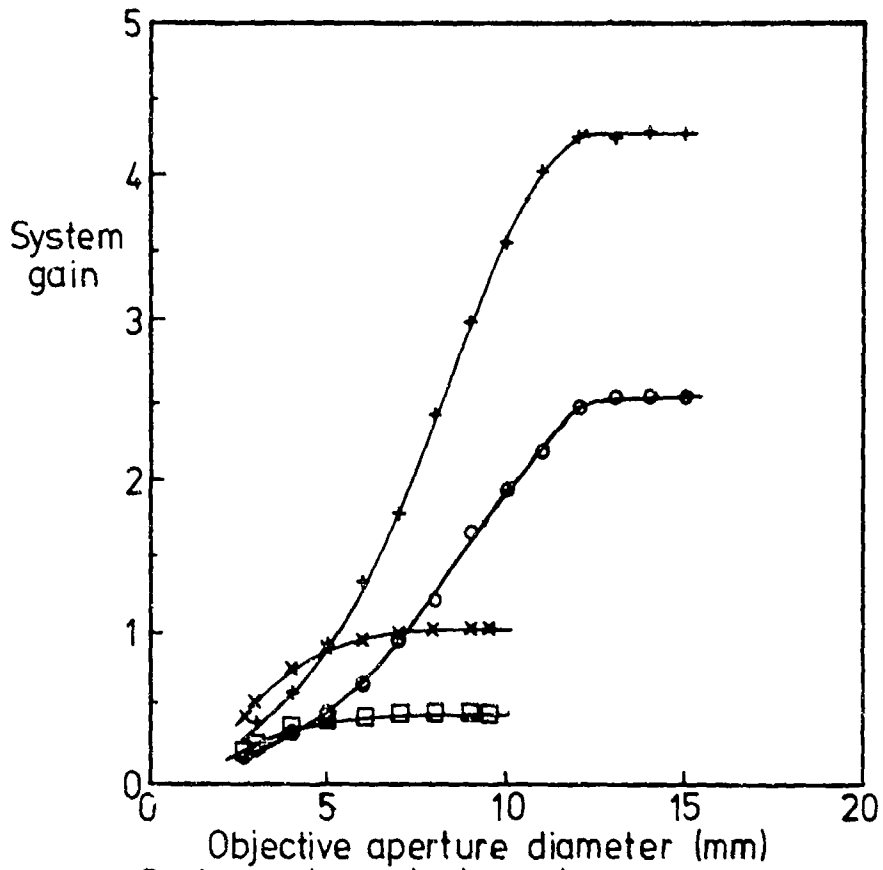


FIGURE 12

System gain against aperture

○ 2x1000 mm Schott fibre bundle, system 2

+ 2x 500

□ 2x1000 " " " " 25 mm lens only

x 2x 500 " " " " " "

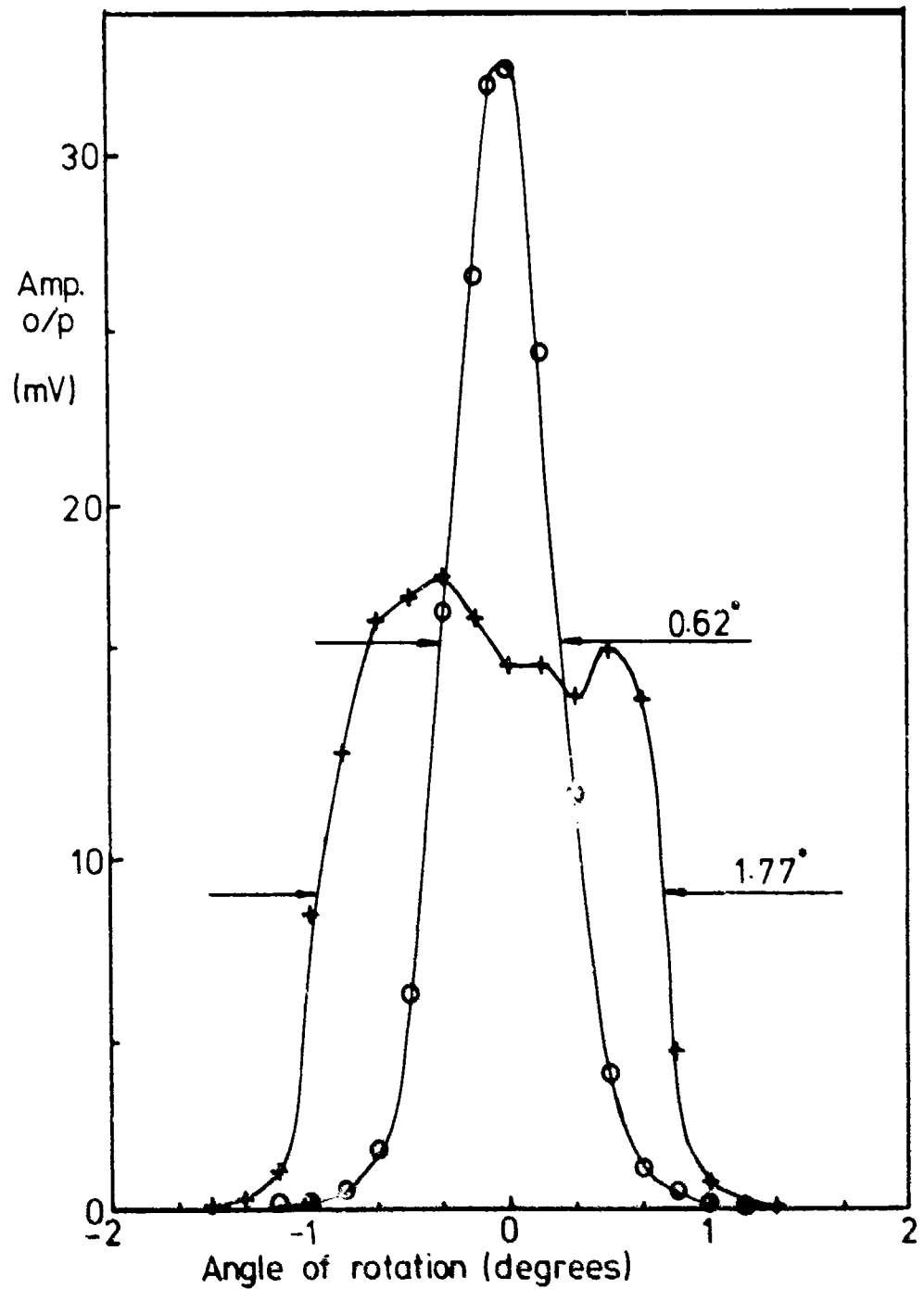


FIGURE 13

Field of view, 214 nm

○ 2 × 500 mm Schott fibre bundle, system 1

+ " " " " .50mm lens only

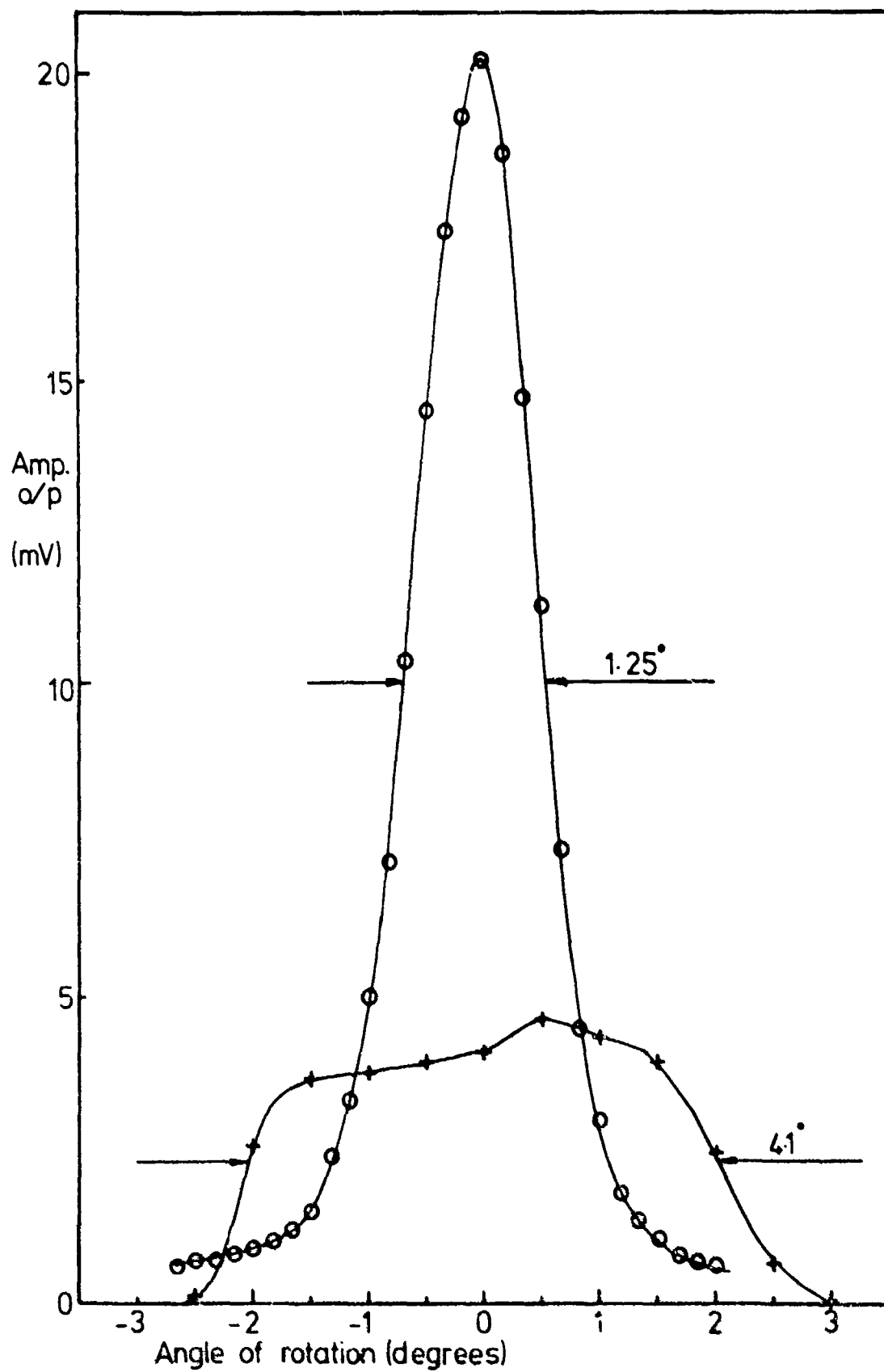


FIGURE 14 Field of view, 214 nm
 o 2x500mm Schott fibre bundle, system 2
 + " " " " " , 25mm lens only

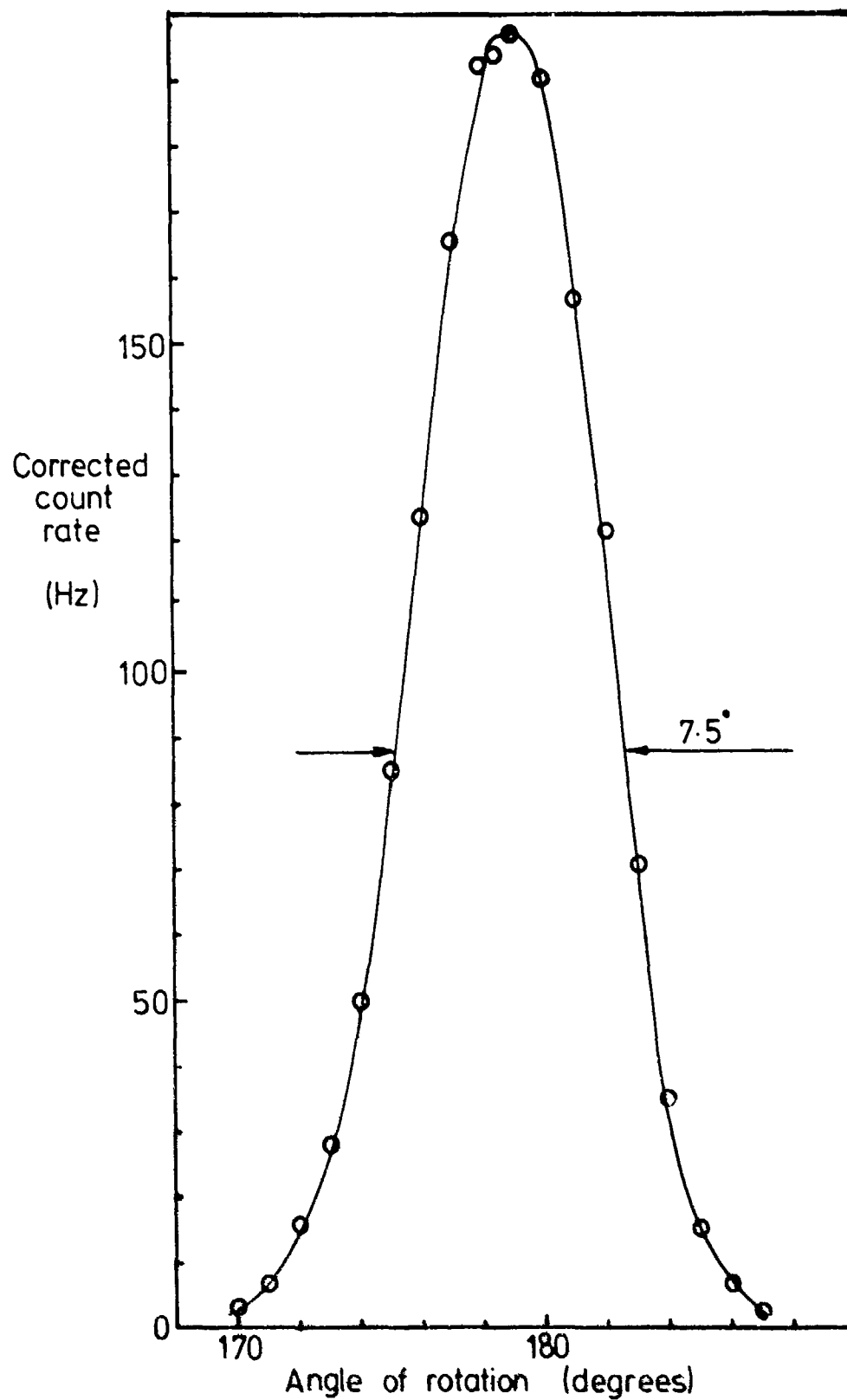


FIGURE 15 Field of view, 214 nm
 2×500mm Schott fibre bundle
 D 6100 detector, 10 mm output lens

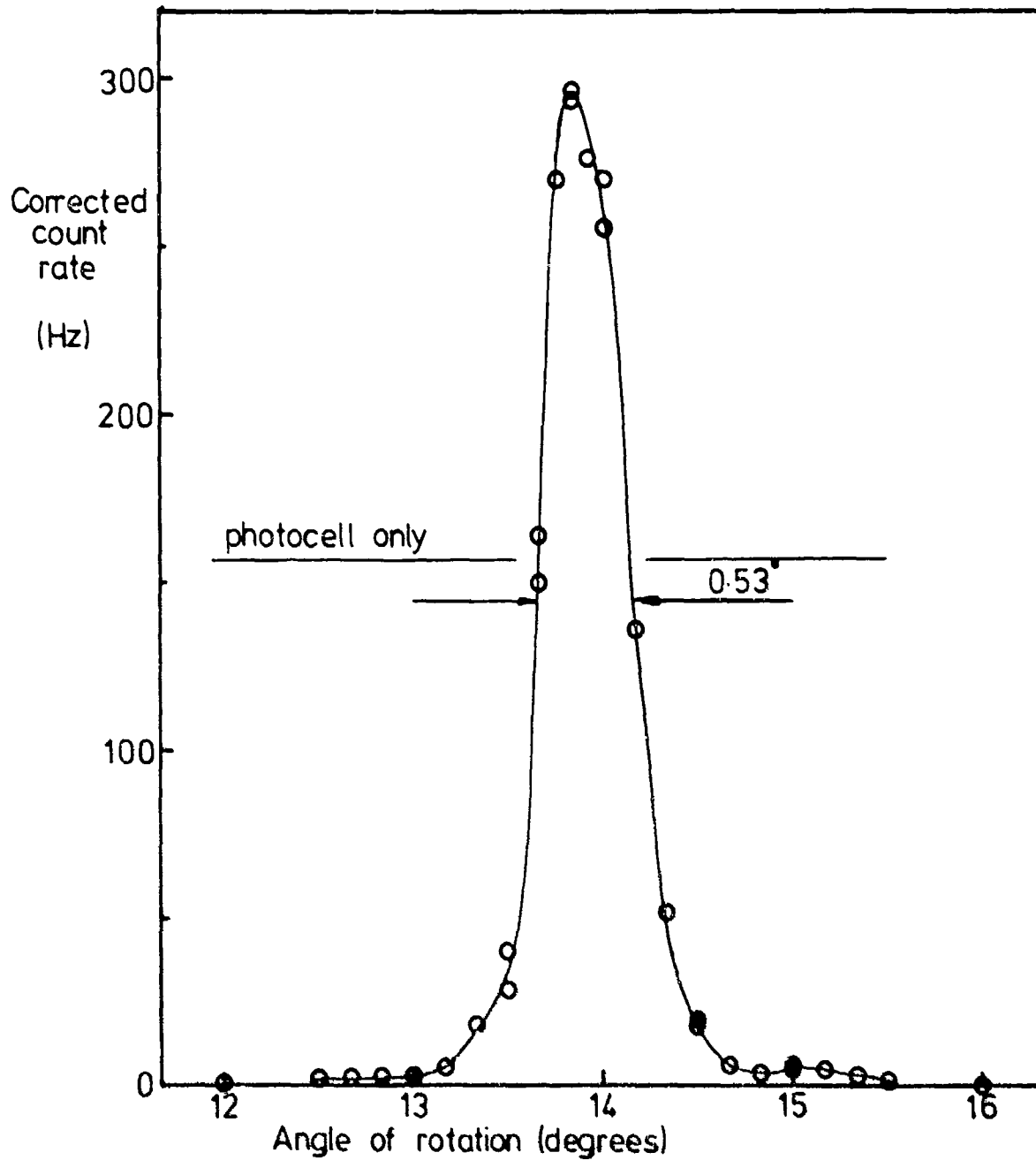


FIGURE 16 Field of view, 214 nm
 2x1000 mm Schott fibre bundle, system 1
 D 6100 detector, 10mm output lens

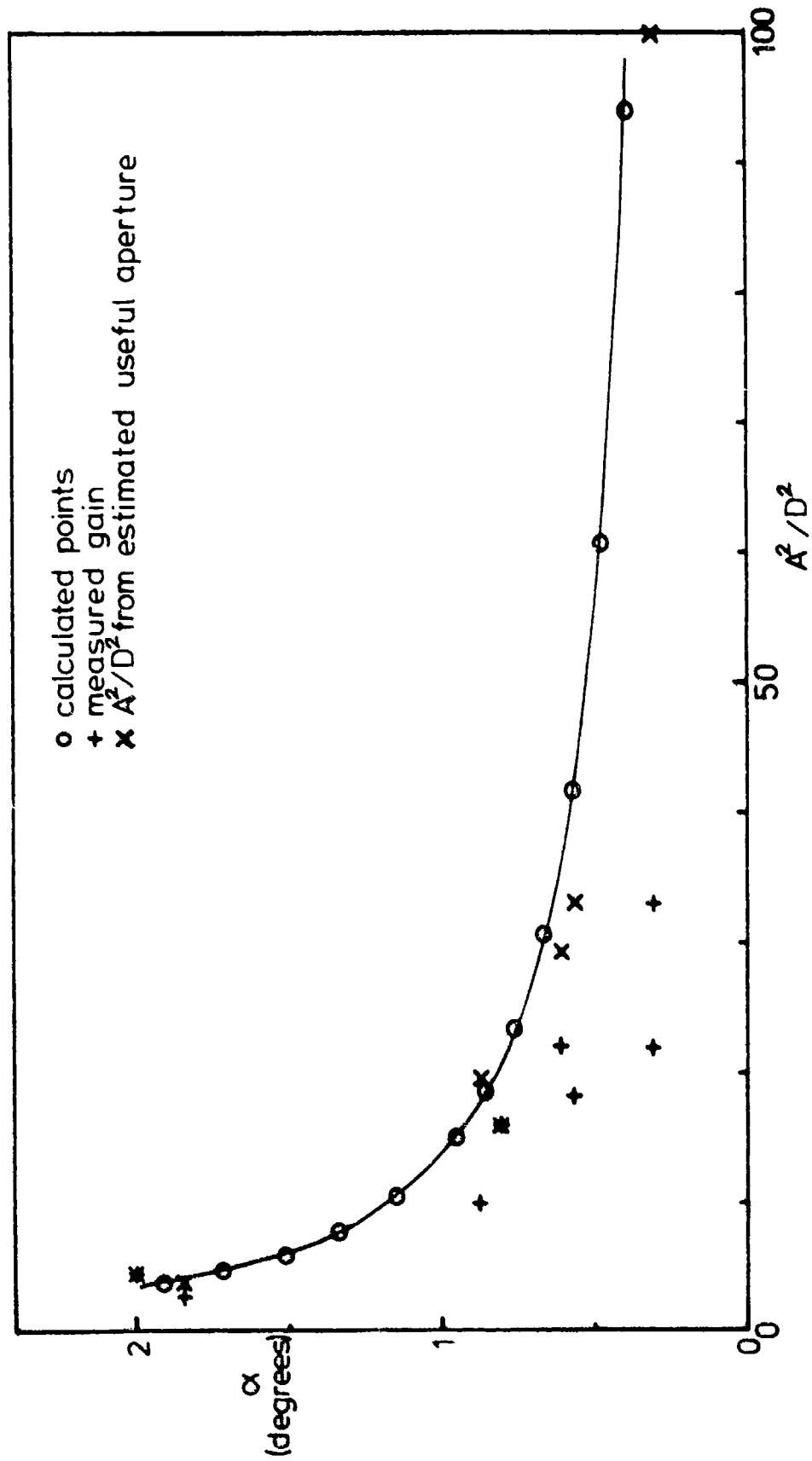


FIGURE 17 FIELD OF VIEW AGAINST GAIN CALCULATED BY THE LAGRANGE INVARIANT FOR A 2x1000mm SCHOTT FIBRE BUNDLE AT 214nm

REFERENCES

1. McGunigle R.D., Jackson H.W. and Beavers R.R.
AFAPL-TR-78-84 Oct. 1978,
"Applicability of Fiber Optics to Aircraft Fire
Detection Systems"
2. Smith W. J.
"Modern Optical Engineering: The Design of Optical Systems",
McGraw-Hill, New York, (1966) pp 230 - 236.
3. Discoll W. G. and Vaughan W.
"Handbook of Optics",
McGraw-Hill, New York, (1978) pp 2 - 8

APPENDIX

MANUFACTURERS DATA SHEETS
SCHOTT - ESKA - QSF

No. 7107

Fibre Optics

Flexible UV Light Guides

Flexible UV Cross-Section

Transformers

UV light conducting fibres are produced by a special technique in which fused quartz fibres are optically insulated with a plastic sheathing. Unlike normal light conductors made entirely of optical glass, they can also transmit ultra violet light at wavelengths down to approximately 250 nm

Flexible UV light guides consist of bundles of the above fibres, the ends being tightly secured in ferrules and the whole being protected from mechanical damage by sheathing

Single, multi-branched, and cross-section transformer light guides can be used to transmit ultra-violet light along a chosen path. Typically they can be used to transmit UV light into inaccessible areas such as those experienced in analysis, measuring techniques and medicine.

Multi-branched light guides have many varied uses. In fluorescent light barriers ultraviolet light can be transmitted by one arm of the light guide and the fluorescent light from the subject guided to the receiver by a second conductor arm.

Standard Type – Technical Data

Fibre:

Type: UV
 Fibre Diameter 100 micron
 Numerical Aperture NA
 and Maximum Aperture Angle $2\alpha_0$
 are dependent on wavelength and light
 guide length:

Wavelength (nm)	Light Guide Length			
	1000 mm		1800 mm	
	NA	$2\alpha_0$	NA	$2\alpha_0$
366	0.26	30.1°	0.21	24.2°
540	0.35	41.0°	0.28	32.5°
860	0.42	49.7°	0.37	43.4°

Types of Sheathing:

Metal

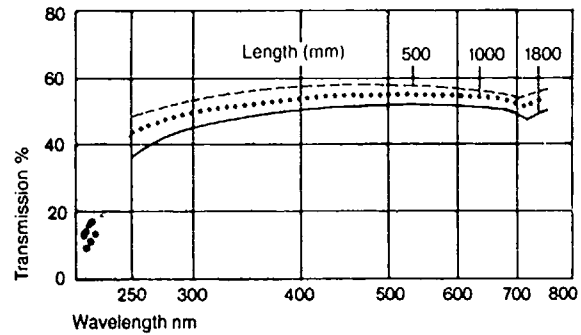
Chrome plated,
 withstand temperature 120°C.

Metal/PVC

Metal sprayed with PVC,
 withstand temperature - 40°C to
 + 80°C

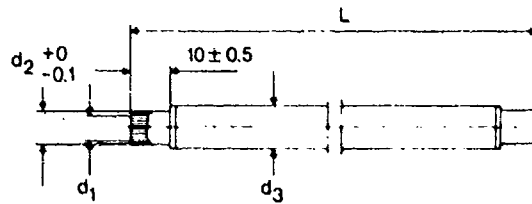
Dimensional Tolerance:

Light Guide Length (mm)	Tolerance (mm)
250, 500	± 10
1000	± 15
1800	± 25



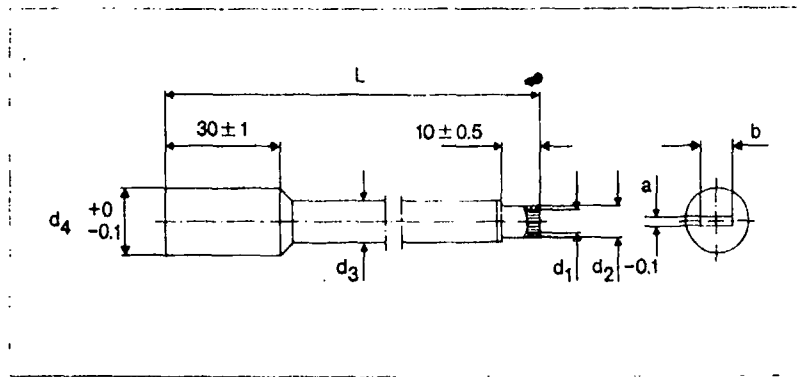
Typical spectral transmission of flexible UV light guides for various lengths.

Single Branch Flexible UV Light Guide



Fibre Bundle Dia d_1 (mm)	Ferrule Dia d_2 (mm)	Sheathing Dia d_3 (mm)		Light Guide Length (mm)			
		Metal	Metal/ PVC	250	500	1000	1800
1	4	6	7	○	○	○	○
2	4	6	7	○	○	○	○
3	4	6	7	○	○	○	○
4	5	7	8	○	○	○	○
5	7	9	10		○	○	○
6	8	10	11		○	○	○
8	10	13	14		○	○	○
10	12	15	16		○	○	○

Flexible UV Cross Section Transformer



MPVC = Metal/PVC Sheathing
M = Metal Sheathing

Cross Section Dimensions*	MPVC					Light Guide Length (mm)			
	a x b	∅ d ₁	∅ d ₂	∅ d ₃	∅ d ₄	250	500	1000	1800
1 x 3	2	4	7	6	10	○	○	○	
1 x 7	3	4	7	6	10	○	○	○	○
1 x 12	4	5	8	7	24		○	○	○
1 x 20	5	7	10	9	24		○	○	○
1.5 x 5	3	4	7	6	10	○	○	○	○
1.5 x 8	4	5	8	7	24		○	○	○
1.5 x 12	5	7	10	9	24		○	○	○
1.5 x 20	6	8	11	10	24		○	○	○
2.5 x 5	4	5	8	7	10		○	○	○
2.5 x 8	5	7	10	9	24		○	○	○
2.5 x 10,5	6	8	11	10	24		○	○	○
2.5 x 20	8	10	14	13	24		○	○	○

* Tolerance to DIN 7168

We reserve the right to make technical alterations.

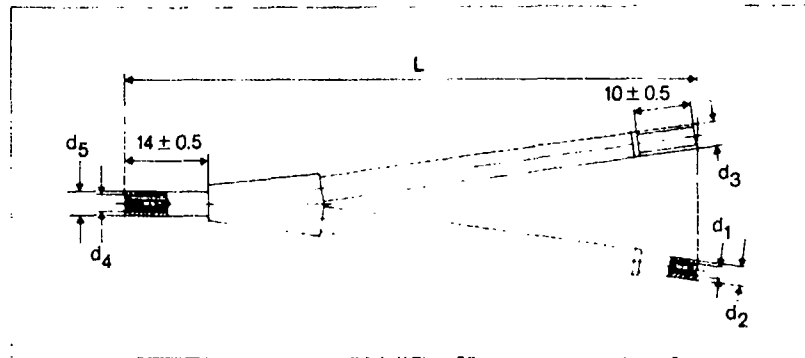
Further details available:

Schott Glass Ltd
Drummond Road
Stafford ST16 3EL
Tel: (0785) 461 31
Telex: 36685

JENAER GLASWERK SCHOTT & GEN
Sales Dept. Fibre Optics
P.O. B. 2480, D-6500 Mainz
Telephone: (061 31) 661
Telex: 4187401 smz d
Cable address: Glaswerk Mainz



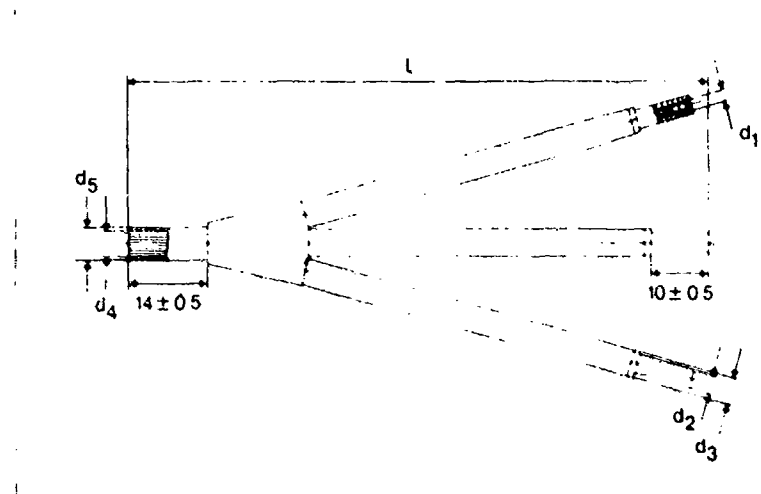
Two Branch Flexible UV Light Guide



Ferrule diameter d_2 and sheathing diameter d_3 are identical to the corresponding dimensions of the single branch flexible light guide (see sheet 2).

Fibre Bundle Dia d_1 (mm)	Fibre Bundle Dia d_2 (mm)	Ferrule Dia d_5 (mm)	Light Guide Length (mm)			
			250	500	1000	1800
1	14	4	○	○	○	
2	28	4	○	○	○	
3	42	6	○	○	○	○
4	57	7		○	○	○

Three Branch Flexible UV Light Guide



Ferrule diameter d_2 and sheathing diameter d_3 are identical to the corresponding dimensions of the single branch flexible light guide (see sheet 2).

Fibre Bundle Dia d_1 (mm)	Fibre Bundle Dia d_2 (mm)	Ferrule Dia d_5 (mm)	Light Guide Length (mm)			
			250	500	1000	1800
1	17	4	○	○	○	
2	35	5	○	○	○	
3	52	7	○	○	○	○
4	69	8		○	○	○

ESKA[®] OPTICAL FIBER AND ASSEMBLED FIBER OPTICS FROM MITSUBISHI RAYON

OF-06

(1) INTRODUCTION

ESKA is the tradename for an acrylic optical fiber and its fabricated products of superior optical properties developed by Mitsubishi Rayon.

ESKA is made of core of acrylic polymer (polymethyl methacrylate) sheathed with a special fluorine containing polymer which has lower refractive index than the core. Light rays input from one end of ESKA travel in a zigzag through ESKA by means of the total internal reflection at core sheath interface and output from the other end.

ESKA bulk fiber and cut bristle are available in diameter from 0.1mm (4mil) to 3mm (120mil). ESKA light conducting cables consist of single bulk fiber or bundle of several bulk fibers, jacketed with black polyethylene of wire cable grade.

An advantage of ESKA product lines is that ESKA is available in the form of assembled fiber optics such as light guides, light sensor heads, line circle converters, photo-couplers and panels and displays. Sample quantity of these assembled fiber optics can be manufactured at our laboratory for testing at customers.

There are two types of ESKA optical fiber: ESKA industrial grade and ESKA II display grade. ESKA industrial grade has excellent optical properties, especially lower loss and less yellowing of transmitted light. It is manufactured and shipped under the strict quality control on its optical and physical properties.

ESKA II display grade has enough optical and physical properties for display uses and is reasonably priced enough to be competitive with other plastic optical fibers.

The advantages of ESKA over glass optical fiber are better flexibility and toughness, lighter weight and easier handling, easier fabrication of assemblies and lower prices.

The advantages of ESKA over polystyrene optical fibers are lower loss of light, less colouring of transmitted light, higher physical properties such as tensile strength and flexibility, better durability such as weathering and heat stability, and easier fabrication.

ESKA has excellent optical and physical properties and durability serviceable in a wide range of end uses from industrial to display uses.

Fig. 1 Structure of Optical Fiber and Path of Light Ray in the Fiber

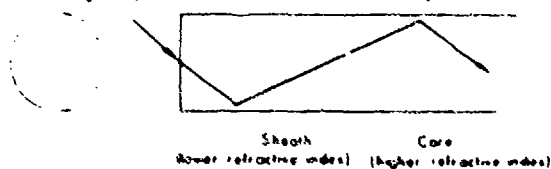
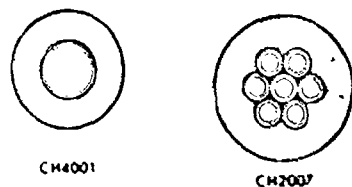


Fig. 2 Cross section of ESKA[®] light conducting cable



(2) TYPES OF ESKA

Bulk Fibers

Industrial Grade ESKA		
Type	Diameter	Meters/Spool
CK-10	0.25mm	8,000m
CK-20	0.5 mm	6,000m
CK-30	0.75mm	2,700m
CK-40	1.0 mm	1,500m

Display Grade ESKA II		
Type	Diameter	Meters/Spool
JK-10	0.25mm	24,000m
JK-20	0.5 mm	6,000m
JK-30	0.75mm	2,700m
JK-40	1.0 mm	1,500m
JK-60	1.5 mm	700m
JK-80	2.0 mm	250m
JK-100	2.5 mm	250m
JK-120	3.0 mm	150m

Fiber Optic Cables

Type	Fiber Dia x No. of Fiber	Outside Dia	Remarks
CH-4001	1.0 mm x 1	2.2 m/m	① Jacketed with Black Polyethylene
CH-2007	0.5 mm x 7	2.8 m/m	
CH-2012	0.5 mm x 12	3.0 m/m	② 500 Meters Pack for All Types
CH-2016	0.5 mm x 16	3.47 m/m	
CH-1016	0.25mm x 16	2.2 m/m	
CH-1032	0.25mm x 32	2.8 m/m	
CH-1048	0.25mm x 48	3.0 m/m	
CH-1064	0.25mm x 64	3.3 m/m	

Cut Bristles

Industrial Grade ESKA		Display Grade ESKA II	
Type	Diameter	Type	Diameter
CK-10C	0.25mm	JK-10C	0.25mm
CK-20C	0.5 mm	JK-20C	0.5 mm
CK-30C	0.75mm	JK-30C	0.75mm
CK-40C	1.0 mm	JK-40C	1.0 mm
		JK-60C	1.5 mm
		JK-80C	2.0 mm
		JK-100C	2.5 mm

Standard Length 500mm Standard No. per bundle 1,500

Fiber Optic Sheets

Industrial Grade ESKA		Display Grade ESKA II	
Type	Diameter	Type	Diameter
CK-10S	0.25mm	JK-10S	0.25mm
CK-20S	0.5 mm	JK-20S	0.5 mm
CK-30S	0.75mm	JK-30S	0.75mm
CK-40S	1.0 mm	JK-40S	1.0 mm

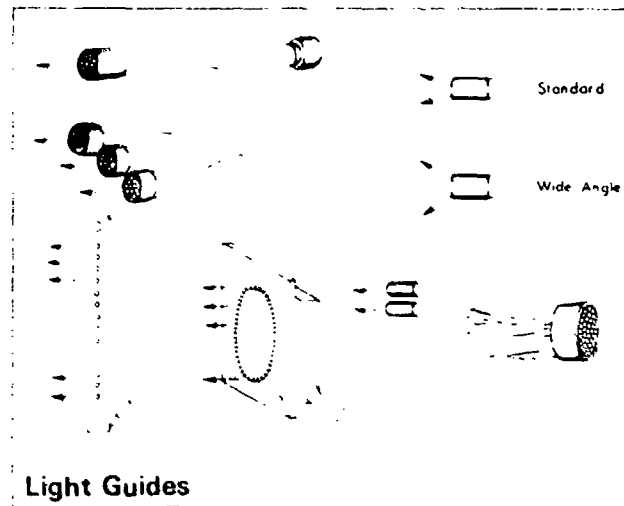
Standard Sheet Size 100mm x 1,000mm

Assembled Fiber Optics

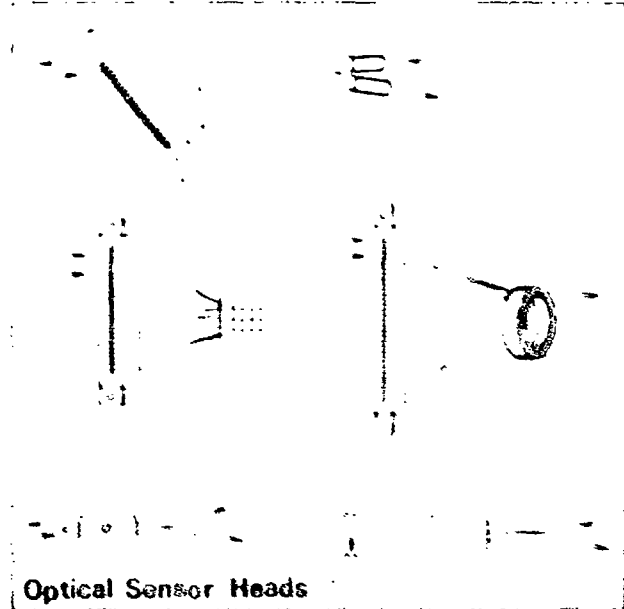
Assemblies of ESKA partly shown in Fig. 2 are available on request.

(3) TYPICAL APPLICATIONS OF ESKA[®]

- A. Light guides
 - safety lighting, without heat and electricity, from remote light source
 - partition of light from one light source
 - pin point lighting
- B. Illumination panels
 - road signs
 - signs at public spaces and pathways
 - control panels
 - simulators
 - panels for exhibitions and the like
 - industrial illumination panels
- C. Automotive
 - illuminations of switches, knobs and other driving instruments on instrument panel
 - illuminations of air conditioner panel and radio set panels
 - illumination of various meters
 - illumination of ash trays and ignition key holes
 - tail light and head light monitors
- D. Electric appliances
 - illuminations of dials, switches, pilot lamps, panels, etc. for radio sets, TV sets and cassette decks
- E. Optical, medical and dental instrumentations
 - lighting devices
 - image guides
 - optical sensors and transducers
- F. Industrial uses and automation
 - optical counting devices for rotations and numbers
 - optical sensing for level, position and distance
 - sensors for color, brightness and turbidities
 - optical sensors for defect inspections
 - other optical sensors and light guides for automations and conveyor lines
 - remote monitoring applications
 - industrial optical data links without electromagnetic noises
- G. Information systems and data processings
 - card and tape reader heads
 - mark, cord and character reader heads
 - line circle converters
 - optical devices for copy machines
 - light pens
 - optical data links
- H. Decoration displays (with ESKA II)
 - decorative lights and X mas tree decoration
 - illuminated displays in water
 - displays in bars and restaurants
 - interior displays
- I. Advertisement displays (with ESKA II)
 - show window displays
 - POP displays
 - eye catchers
 - displays of trade names and marks
- J. Assembly kits and toys (with ESKA II)
 - assembly kits of illuminated flowers and decorative lights
 - illumination in plastic models
 - illumination in toys such as vehicles, robots and animals
 - games and puzzles



Light Guides



Optical Sensor Heads

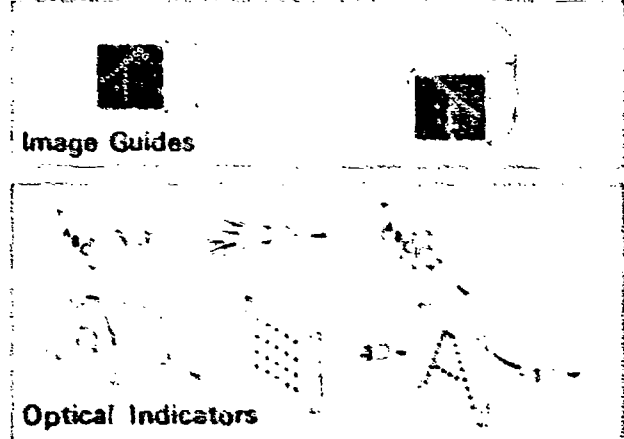


Image Guides

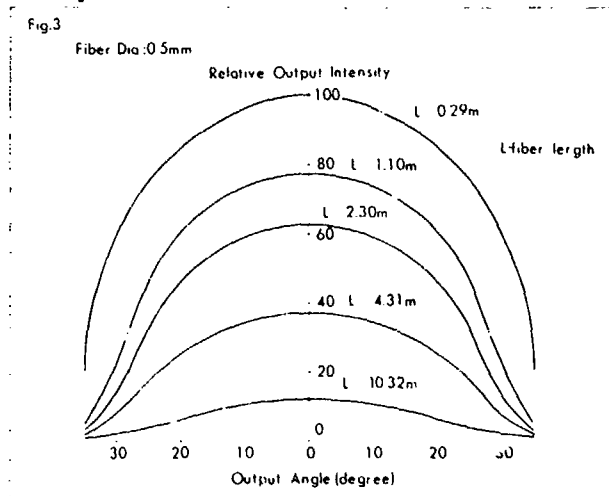
Optical Indicators

(4) OPTICAL PROPERTIES OF ESKA[®]

Numerical Aperture, Acceptance Angle

Core Refractive Index 1.495 (n₁)
 Sheath Refractive Index 1.402 (n₂)
 Numerical Aperture (N.A.) 0.50 (N.A. = $\sqrt{n_1^2 - n_2^2}$)
 Acceptance Angle 60° (Acceptance Angle = $2\text{Sin}^{-1}(\text{N.A.})$)

Relative Output Intensity vs. Output Direction



Transmission vs. Bend Radius

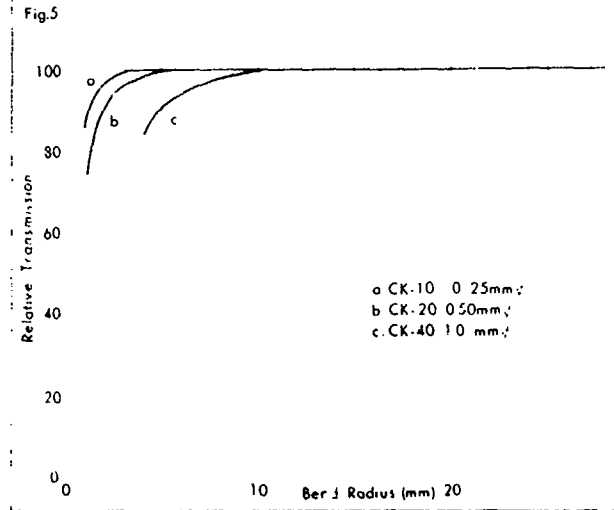
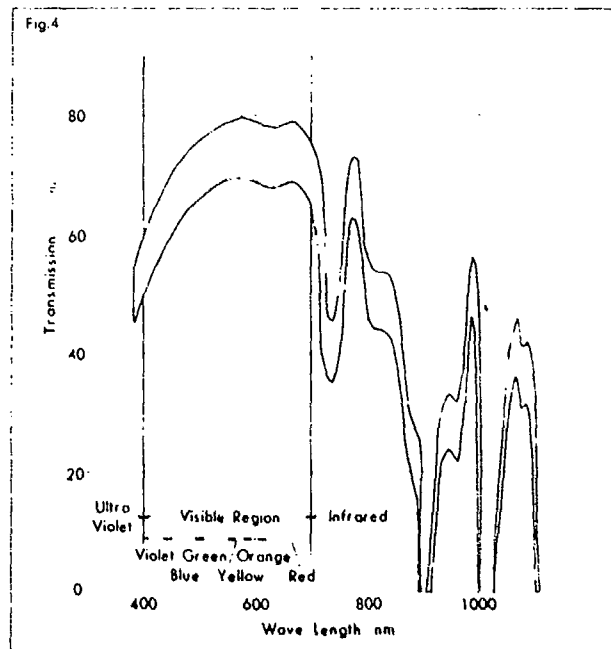


Fig. A
 * Bend Angle: 180
 Temperature: RT
 Fiber Length: 1.5m

Spectral Transmission



Advantages of ESKA[®] in Optical Properties

- (a) Lower loss of light, or transmission of light over longer distance.
- (b) Less colouring of transmitted light.
- (c) High, uniform transmission through the whole visible region of spectrum.

These advantages of ESKA are largely attributable to the improvements in optical purity of core polymer, and designing of sheath polymer and the construction of sheath core interface. All individual fibers of ESKA industrial grade are produced under the special quality control procedures including non-destructive light transmission test.

(5) PHYSICAL PROPERTIES OF ESKA®

Breaking Stress and Strain

Table 1

Type	Fiber Dia.	Breaking Stress		Young's Modulus		Breaking Strain	
		kg Fiber	kg/cm ²	10 ⁹ kg/cm ²	10 ⁹ kg/cm ²		
CK-10	0.25mm	0.5	0.55	1200	1300	3.9-4.0	50-60
CK-20	0.50mm	1.6	2.0	900	1100	3.0-3.6	50-80
CK-40	1.0mm	5.7	7.0	700	900	2.7-2.9	50-80
CH-4001	1.0mm-PE	11	13				50-70

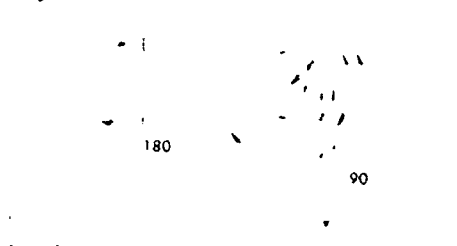
Flexibility

Table 2

Type	Fiber Dia.	Bend Radius (mm)	Bend Angle (degree)	Relative Light Transmission after 100 Bends	
				at 90°	at 180°
Bulk Fiber	0.25mm	6	90	100	100
Fiber Optic Cable	CH-4001	6	90	100	100
			180	100	100

Temperature: R.T. Bending Cycle: 1 bend/sec

Fig B



Weatherability

There were no noticeable changes in light transmission and physical properties of ESKA after 200 hr. exposure by weather-O-meter.

Chemical Resistance

Table 3 Relative Light Transmission

	Condition	Bulk Fiber (CK-20)		Fiber Optic Cable (CH-4001)	
		100%	m(30days)	100%	m(30days)
Water	(R.T.)	100	m(30days)	100	m(30days)
	(60°C)	100	m(30days)	100	m(30days)
Boiling Water		80	m(10days)	90	m(10days)
Machine Oils(R.T.)				100	m(10days)
Diluted Sulfic Acid (-)				100	m(10days)
Gasolines (-)		Decrease		100	m(5days)
Organic Solvents				100	m(5days)
Acetone, Ethyl Acetate, Benzene, etc.		Decrease		100	m(5days)

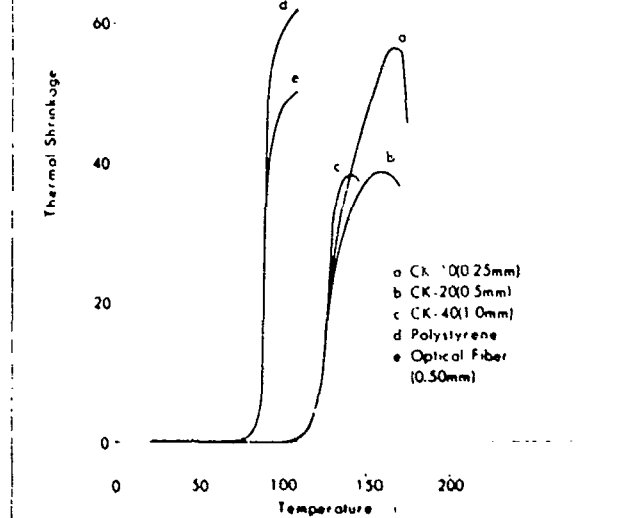
On condition that the jacket can resist these organic solvents.

High-and low-temperature resistance

While intermittent exposures to temperatures of around 100°C can be tolerated, the maximum continuous service temperature is limited up to around 80°C because of slight thermal shrinkage thereabove. (Fig. 6)

There was no change in light transmission of ESKA after the low temperature test at -30°C for 30 days, and ESKA retains flexibility even at -30°C. No cracking at low temperature bending test, down to -30°C.

Fig. 6 Thermal Shrinkage as a Function of Temperature heating rate 1 min./load 2g



Advantages of ESKA® in Physical Properties.

- ESKA has high flexibility and toughness through a wide range of temperature. As an illustration of its flexibility, it can be knotted tightly at room temperature.
- ESKA possesses higher durability in terms of thermal resistance, weatherability and chemical resistance than polystyrene optical fibers.
- ESKA is not attacked by epoxy adhesives.

Optronics Ltd

CAMBRIDGE SCIENCE PARK

MILTON ROAD

CAMBRIDGE

ENGLAND CB4 4BH

Tel CAMBRIDGE (0-231) 64364/5

.,LTD.

JAPAN

QSF series low-loss, large diame

Quartz & Silice

own production of high purity fused silica is used for the manufacture of **FIBROPSIL fibres**. Maximum uncut length of fibre is greater than that obtainable from any other source
Typical attenuation is < 5 dB/Km (820 nm)

The high homogeneity of core material combined with the unique drawing procedures ensure the high tensile strength of **FIBROPSIL fibres**.

The rugged extruded coating offers unequalled flexibility in fibre handling

Radiation resistance is very high, and has been confirmed in independent government trials to be better than all other available fibres

- Lowest loss of all PCS fibres
- High numerical aperture
- High tensile strength and flexibility
- Excellent radiation hardness
- Extremely long uncut length
- High power handling capabilities with superlarge cores
- Best coupling efficiency with superlarge cores
- Ideal for UV and IR light transmission
- New improved tolerances
- New improved low temperature capability

Recent advances in the drawing technique have enabled the guarantee of $\pm 4\%$ core tolerance, with the added capability of $\pm 2\%$ on special order. The continual investigation of new materials have led to a

low temperature PCS fibre. For applications down to -55°C , **FIBROPSIL fibres** are available on special order with limited attenuation increase, exhibiting no optical cutoff (ref : QSF-LT.)

Trade	QSF 125			QSF 200			QSF 300			QSF 400		QSF 600		QSF 1000		Notes
Numbers	A	B	C	A	B	C	A	B	C	A	C	A	C	A	C	
Core diameters μm	125			200			300			400		600		1000		1
Standard silicone resin coating μm	300			380			440			550		750		1250		2
Standard Tetral [®] coating μm	420			600			650			650		1060		1550		3
Max uncut length km	25			25			12			5		3		1		4
Attenuation Max dB/km 0,82 Typ	5,5	10	50	<5	<10	<50	5	10	50	5	50	5	50	5	50	5
	5	8	30	4,8	7	30	4,5	6	25	3,5	25	3	25	3	25	3
NA Theoretical	0,40			0,40			0,40			0,40		0,40		0,40		6
Steady state	0,27			0,27			0,27			0,27		0,27		0,27		6
Typical bandwidth MHz/1 km (NA 0,3)	30			25			20			15		9				7
Minimum bend radius mm	2			3			10			12		15		25		
Weight kg/100m	0,210			0,490			0,860			1,250		1,950		3,900		

All fibres are proof tested at a minimum tensile strength of 25000 psi (17,3 daN/mm)

ter, silica cores

The high NA and low attenuation combine to provide higher power output than for all-glass fibres.

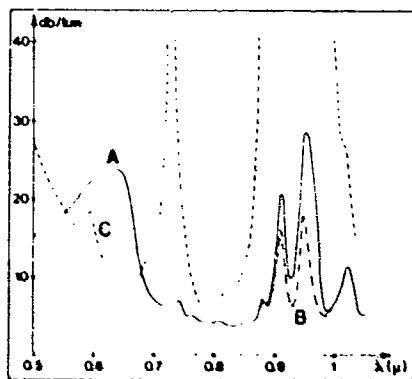
The superlarge core **FIBROPSIL fibres** (400 - 1500 core diameter) have all

of above advantages and in addition display high power throughput capability (> 100 watts). Thus they find applications in laser surgery and in weapons/explosives research. The excellent filling coefficient and the superior UV/IR transmission

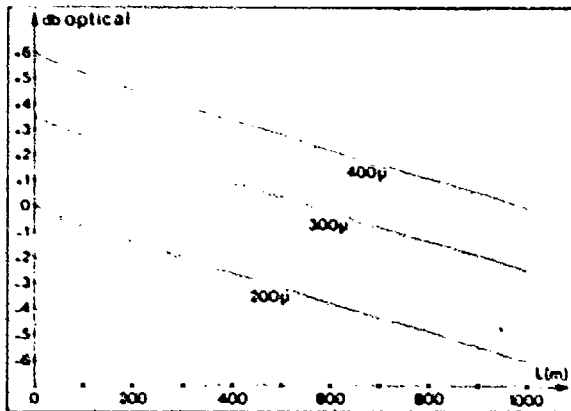
of pure silica allow replacement of fibre bundles with improved performance.

Notes

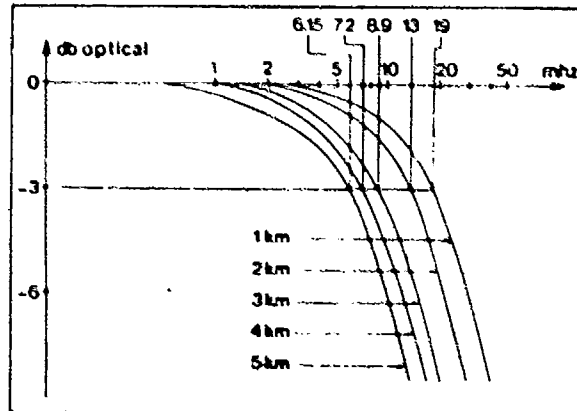
1. Core diameter tolerance $\pm 4\%$
2. Cladding diameter tolerance $\pm 8\%$
3. Core, cladding and coating dimensions may be modified upon request to suit specific requirements.
4. Fibres are currently shipped on a polystyrene reel with 325 mm barrel diameter and 100 mm traverse. Fibres QSF 125-200-300 can be shipped on a plastic reel (DIN 8559) with 212 mm barrel diameter and 91 mm traverse. Fibres can be crosound with each end marked and accessible with a minimum attenuation increase.
5. Attenuation measurement is determined by comparing the transmitted light power through two different fibre lengths.
6. Theoretical NA (calculated at 20 °C) = $\sqrt{(1.4585)^2 - (1.405)^2} = 0,391 \approx 0,4$. Steady state NA measured at the 90 % power output level on 1 Km length.
7. Fibre bandwidth is determined by using a frequency domain approach and is specified at the 3 dB optical power point on the fibre frequency response plot.



Typical attenuation VS wavelength
 A standard QSF A
 B superdry QSF A (upon request)
 C wet QSF A (upon request)



Typical effective power output when launching NA is greater than theoretical NA. Attenuation is 4 db/km at 0.82 μ. Reference level (0 db) was chosen for QSF 200 A at 0 meter length



Attenuation/Bandwidth characteristic of QSF 200 A, 0.27 N.A. input.